# CHARACTERISTICS OF DIVERTOR PLASMA IN NEUTRAL BEAM HEATED ASDEX DISCHARGES

Y. Shimomura[+], M. Keilhacker, K. Lackner
H. Murmann, G. Siller

IPP III/80 December 1982

MAX-PLANCK-INSTITUT FÜR PLASMAPHYSIK
8046 GARCHING BEI MÜNCHEN

**MAX-PLANCK-INSTITUT FÜR PLASMAPHYSIK**

**GARCHING BEI MÜNCHEN**

# CHARACTERISTICS OF DIVERTOR PLASMA IN NEUTRAL BEAM HEATED ASDEX DISCHARGES

Y. Shimomura[+], M. Keilhacker, K. Lackner
H. Murmann, G. Siller

IPP III/80 December 1982

[+]Japan Atomic Energy Research Institue,
Naka-macki, Naka-gun, Ibaraki-ken, 311-62, JAPAN

*Die nachstehende Arbeit wurde im Rahmen des Vertrages zwischen dem Max-Planck-Institut für Plasmaphysik und der Europäischen Atomgemeinschaft über die Zusammenarbeit auf dem Gebiete der Plasmaphysik durchgeführt.*

Contents

IPP III/80

Y. Shimomura[+]
M. Keilhacker
K. Lackner
H. Murmann
G. Siller

# CHARACTERISTICS OF DIVERTOR PLASMA IN NEUTRAL BEAM HEATED ASDEX DISCHARGES

December 1982
(in English)

## Abstract

Characteristics of divertor plasma with neutral beam injection ($P_{NI} \leq 2.5$ MW) are studied. Major objectives are obtaining an ideal divertor plasma with low temperature and high density as well as clarifying plasma characteristics in the divertor. The major conclusions are as follows:

1. A strong inhomogeneity along magnetic field lines of density, $n_e$, and temperature, $T_e$, in the scrape-off layer, e.g. $T_{eb} \sim 100$ eV and $n_{eb} \sim 10^{13}$ cm$^{-3}$ at the torus mid-plane in the main chamber and $T_{ed} \sim 10$ eV and $n_{ed} \sim 10^{14}$ cm$^{-3}$ near the neutralizer plate in the divertor chamber.

2. Plasma parameters near the neutralizer plate such as $T_{ed}$ and $n_{ed}$ are strong functions of recycling conditions in the divertor, e.g. gas source, pumping speed and width of divertor throat, as well as of discharge conditions in the main chamber, e.g. density, heating power and confinement.

3. The electron temperature $T_{ed}$ near the neutralizer plate is a strong function of the electron density $n_{ed}$ near the neutralizer plate and the heating power, i.e. $T_{ed}$ decreases with increasing $n_{ed}$ and with reducing the heating power.

4. At a very low value of $T_{ed}$, when the ionization coefficients of hydrogen are very small, the divertor plasma cannot stop a strong neutral gas backflow from the divertor chamber into the main chamber and disruptions are induced. Thus, the minimum value of $T_{ed}$ is around 5 eV and the maximum value of $n_{ed}$ is obtained at around $T_{ed} = 5$ eV in a stable discharge. The maximum value of $n_{ed}$ at the minimum $T_{ed}$ is proportional to the heating power $P_{OH} + P_{NI}$.

5. An ideal divertor plasma with low temperature and high density is obtained in a stable discharge with neutral beam injection. For example, $T_{ed}$ is maintained at a low value of 7 eV by an increase of $n_{ed}$ from $10^{13}$ $cm^{-3}$ to $1.2 \times 10^{14}$ $cm^{-3}$ when the heating power $P_{OH} + P_{NI}$ is raised from 0.35 to 2.5 MW while keeping the main plasma density fixed at $7 \times 10^{13}$ $cm^{-3}$.

## 1. Introduction

ASDEX /1/ is a large tokamak (R = 1.65 m, a = 0.4 m, $B_t \leq 2.8$ T, $I_p \leq 500$ kA) with a double-null poloidal divertor. The bulk plasma is confined magnetically in the main chamber and charged particles lost from the bulk plasma flow in a narrow scrape-off layer along field lines into the divertor chamber. Thus major plasma-wall interactions are restricted to the divertor chamber. Successful impurity control is demonstrated with neutral beam injection of 3 MW in ASDEX /2/ as was already shown earlier in DIVA for ohmic heating powers of up to 0.3 MW /3/. Also, neutral beam injection into diverted ASDEX discharges reveals a new operational regime with high $\beta_p$ and good confinement times /4/. The poloidal divertor, therefore, is a promising impurity control method for tokamaks.

In order to apply a poloidal divertor to a reactor grade device, two major problems must be overcome, i.e. simplifying the divertor configuration /5/ and cooling the diverted plasma near the neturalizer palte /6/. The later problem is studied in this paper. Cooling the diverted plasma is essential to avoid the serious erosion of the neutralizer plate, as well as to reduce the high heat flux density. The temperature $T_{ed}$ near the neutralizer plate has to be very low, typically 10 eV or a less value. Energy and particle conservation laws give the following simple formula for $T_{ed}$ with a normal sheath /3/.

$$T_{ed} = \frac{\bar{\tau}_p}{\tau_E} \cdot \frac{3}{\gamma} \cdot \frac{P_{in} - P_r}{P_{in}} \cdot \bar{T} \qquad (1)$$

Here $P_{in}$, $P_r$, $\bar{T}$, $\tau_E$, $\bar{\tau}_p$ and $\gamma$ are heating power, radiation loss power including charge exhcange loss, mean temperature in the main plasma, energy confinement time, global particle confinement time, and heat transmission rate at the limiter or the neutralizer plate. In the small scale device DIVA /3/, $\bar{\tau}_p$ is almost equal to the particle confinement time $\tau_p$ in the

main plasma and $P_r$ comes only from the main plasma. Therefore $\bar{\tau}_p/\tau_E \sim 1$ and $P_r < 0.5\ P_{in}$. $\gamma \lesssim 10$ from the normal sheath model and also from the experimental results. These values give $T_{ed} > 0.15\ \bar{T}$. If this scaling is applied to a large device, $T_{ed}$ should be very high causing serious problems (high erosion rate and high heat flux density) /6/.

In a large device, we have the possibility of a strong inhomogeneity along magnetic field line isolating the diverted plasma from the main plasma /7/. In this case $\bar{\tau}_p$ may be strongly reduced by increasing particle source or recycling only in the divertor ($\bar{\tau}_p \ll \tau_E$ or $\tau_p$) and $P_r$ may also be increased only in the divertor ($P_r \lesssim P_{in}$) /8/ thereby strongly reducing $T_{ed}$. Experimental results from ASDEX /1/ and Doublet III /9-11/ suggest these possibilities. They have shown a significant enhancement of the neutral gas pressure and the scrape-off layer plasma density in the divertor. In addition, strong radiation, e.g. 100 - 300 kW, was observed only from the divertor. These results were obtained only from high density discharges. In these studies, plasma parameters in the divertor, especially $T_{ed}$, were not measured, characteristics of the plasma were not known, no active control of the divertor plasma was studied and no additional heating was applied. Thus it becomes important to study the influence of strong inhomogeneities along the magnetic field lines on the divertor plasma, in particular for the case of intense additional heating.

In recent ASDEX experiments with neutral beam injection, $P_{NI} \leq 2.5$ MW, characteristics of the divertor plasma were investigated. Plasma parameters in the divertor were measured under a wide range of discharge conditions with a strong inhomogeneity along magnetic field lines present. Density and temperature limits were studied and cooling of the divertor plasma was demonstrated. Some of these results have been reported in Ref. /2/. Detailed studies are given in this paper.

Typical plasma parameters in the divertor are shown in the following section. In section 3, strong temperature and density gradients along magnetic field lines are demonstrated by comparing parameters at the torus mid-plane to those near the divertor plate. In section 4, control of the divertor plasma at low temperature with $0.0 < P_{NI} < 2.5$ MW is described. In section 5, the lower limit of electron temperature and the upper limit of plasma density in the divertor are shown, and disruptions induced by strong gas back flow from the divertor into the main chamber are discussed. Discussions of divertor plasma characteristics are given in section 6. A summary is given in the last section.

## 2. Typical plasma parameters near the divertor plate

Electron temperature and density profiles of the divertor plasma are measured by scanning Langmuir probes near the divertor plate (Fig. 1) under a wide range of discharge conditions[+)]. In Fig.2, typcial profiles of ion saturation current $i_s$ and electron temperature $T_{ed}$ are shown for rather low density discharges with 2.5 MW neutral injection and ohmic heating, respectively. Both temperature and ion saturation current are larger with neutral injection. Relative values of electron density are calculated from $i_s$ and $T_{ed}$. The absolute calibration is made by using the cut-off density of μ-waves (see Appendix).

The peak density $n_{ed}$ and the peak temperature $T_{ed}$ of the profiles near the divertor plate with and without neutral beam injection are shown in Fig. 3. In this epxeriment only the main plasma density $\bar{n}_e$ is scanned, while keeping other discharge parameters constant. The following three regions are observed in both discharges with and without neutral beam injection. The density $n_{ed}$ increases slowly with increasing main plasma density $\bar{n}_e$ at low plasma densities ($\bar{n}_e < 3 \times 10^{13}$ $cm^{-3}$ with $P_{NI} = 0$ and $\bar{n}_e < 5 \times 10^{13}$ $cm^{-3}$ wtih $P_{NI} = 2.5$ MW). In a medium density region ($3.5 \times 10^{13}$ $cm^{-3} < n_e < 4.5 \times 10^{13}$ $cm^{-3}$ with $P_{NI} = 0$ and $5 \times 10^{13}$ $cm^{-3} < \bar{n}_e < 8 \times 10^{13}$ $cm^{-3}$ with $P_{NI} = 2.5$ MW), $n_{ed}$ increases steeply with increasing main plasma density $\bar{n}_e$. In the high density region ($\bar{n}_e > 5 \times 10^{13}$ $cm^{-3}$ with $P_{NI} = 0$ and $\bar{n}_e > 8 \times 10^{13}$ $cm^{-3}$ with $P_{NI} = 2.5$ MW), $n_{ed}$ saturates or decreases. The absolute value of $\bar{n}_e$ for each region changes with changing discharge conditions, especially the heating and recycling conditions as discussed later. The characteristics of the three regions, however, do not change and qualitatively agree with recent numerical results /7/. Without neutral beam injection, the first region was observed in DIVA /3/ and the first and the second regions were observed in ASDEX /1/ and

---

[+)] If not stated differently the following operating conditions were being used: Filling gas $D_2$, $H^0$ beam, $B_t = 2.17$ T, double null divertor (vertical displacement of the plasma column = 0 cm), divertor throat with minimum width of 5.5 cm and $I_M/I_p = 0.1$ ($I_M$: multi-pole coil current, $I_p$: plasma current).

D-III /9-10/. The third region, where $n_{ed}$ saturates or decreases with increasing $\bar{n}_e$, shows the density limit in the divertor. In this experiment, the maximum value of $n_{ed}$ is $1.8 \times 10^{13}$ cm$^{-3}$ at $\bar{n}_e = 5.5 \times 10^{13}$ cm$^{-3}$ with $P_{NI} = 0$ and $1.3 \times 10^{14}$ cm$^{-3}$ at $\bar{n}_e = 9 \times 10^{13}$ cm$^{-3}$ with $P_{NI} = 2.5$ MW. Thus a high divertor density, in excess of the main plasma density, can be obtained. Electron temperatures $T_{ed}$, also shown in Fig. 3, are in the range 5 - 30 eV. $T_{ed}$ is reduced with increasing $\bar{n}_e$ or $n_{ed}$. The peak position of the profiles is discussed in the Appendix.

## 3. Inhomogeneity along magnetic field lines

In order to understand characteristics of the scrape-off layer plasma along magnetic field lines, electron density $n_{eb}$ and temperature $T_{eb}$ profiles in the torus mid-plane are measured with a Thomson scattering system and are compared with the profiles in the divertor. The radial temperature fall-off length at the torus mid-plane $\lambda_{Te}$ is very short, i.e. $\lambda_{Te} \lesssim 1$ cm. Therefore the exact position of the separatrix surface, i.e. the boundary between the main plasma and the scrape-off layer, cannot be obtained with high accuracy. It is impossible to compare plasmas at the torus mid-plane with divertor plasmas along each flux surface by using only geometrical relations. In this paper, we assume $n_e T_e$ = constant on a magnetic surface and adjust the two electron pressure profiles by moving the position of the separatrix magnetic surface at the torus mid-plane. Geometrical factors shown in the Appendix are employed. Adjusted pressure profiles are shown in Fig.4. Radial profiles of $T_{ed}$, $n_{ed}$, $T_{eb}$ and $n_{eb}$ are shown in Fig. 5. Temperature and density inhomogeneities along magnetic field lines are observed in all cases, particularly in the high current discharge with $P_{NI}$ = 2.5 MW, where the electron temperature is reduced by a factor of 10 and the density increased by a factor of 10.

## 4. Control of divertor plasma

Because of the strong inhomogeneities along the plasma flow in the scrape-off layer, the possibility exists of controlling the divertor plasma without changing the main plasma parameters. The most reliable method of changing the divertor plasma condition is by controlling the particle recycling. The following situations have been studied:

- Pumping (Ti gettering) in the divertor (DP operation)
- No pumping in the divertor (D operation)
- Gas puffing in the divertor (DG operation)
- Narrowing the divertor throat (DN operation)

In an ohmic DP discharge, $T_{ed}$ is sufficiently low for rather high densities ($\bar{n}_e = 7 \times 10^{13}$ cm$^{-3}$) in the main chamber (see for example Fig. 10). With 2.5 MW neutral beam injection, $T_{ed}$ increases to 17 eV while the density remains constant as shown by (O) in Fig.6. With more heating power $T_{ed}$ would be further increased, finally to values that are not suitable for divertor operation. The temperature $T_{ed}$ can be reduced by increasing the particle source in the divertor. For example, when particle recycling is increased by stopping titanium gettering (D operation), $T_{ed}$ is reduced to 10 eV or less as shown by (●) in Fig.6. If a lower temperature is required, an additional particle source can be created by puffing gas into the divertor chamber (DG operation), as shown by (⊛) in Fig. 6. Besides the H or HL-type discharges Fig. 6 also shows an example of L-type discharges.

Applying these methods we can maintain the electron temperature $T_{ed}$ at a low value even if the heating powr is increased. This result is shown in Fig. 7. The main plasma density $\bar{n}_e$ is kept constant at around $7 \times 10^{13}$ cm$^{-3}$. When the heating power is increased from 0.3 MW to 2.5 MW, $T_{ed}$ stays at around 7 eV, while $n_{ed}$ increases from $1 \times 10^{13}$ cm$^{-3}$ to $1.3 \times 10^{14}$ cm$^{-3}$. With $P_{NI} = 2.5$ MW, the electron density $n_{ed}$ near the divertor plate

is almost two times higher than the main plasma density $\bar{n}_e$. It is this high density which cools the plasma, thus allowing a sufficiently low value of $T_{ed}$. An example of the plasma profile near the divertor plate for such a high density divertor plasma is shown in Fig. 8.

By narrowing the divertor throat (DN operation), the density in the diverotr can be increased because of a reduction of particle back flow into the main chamber. This effect is shown in Fig.21.

## 5. Density and temperature limits in the divertor

The electron temperature $T_{ed}$ is reduced by increasing $n_{ed}$ as discussed in the previous section. It is very interesting to know the minimum value of $T_{ed}$ or the maximum value of $n_{ed}$ which can be obtained. It is also very important to test the possibility of a gas neutralizer /12/. (In this proposed idea $T_{ed}$ is very low, typically around 1 eV, recombination processes become dominant in the divertor, and no divertor plate is necessary thus avoiding the thermal problems connected with the divertor plate).

In order to obtain a minimum $T_{ed}$, $n_{ed}$ is increased by increasing the main plasma density $\bar{n}_e$. Time variations of the double probe current ($i_s$) at the peak position, the main plasma density, and other parameters are shown in Fig. 9. In this case, the magnetic configuration achieves a steady state 0.6 sec after starting the discharge and the mean plasma density increases from $\bar{n}_e = 7 \times 10^{13}$ cm$^{-3}$ at 1.35 sec. With increasing $\bar{n}_e$, ion-saturation current increases in the early phase, saturates in the meadium phase and decreases in the last phase of the discharge. The electron temperature $T_{ed}$ is monotonically reduced as shown in Fig. 9 (2) and (3). This experiment was performed for a variety of discharge conditions such as gas influx rate, recycling condition, and heating power. Some results for ohmically heated plasmas are summarized in Fig. 10.

The observed minimum temperature for a stable discharge is around 5-6 eV. Below this value, the discharge can easily go into a disruptive phase. At $T_{ed} \sim 6$ eV, $n_{ed}$ is saturated. In some cases, $n_{ed}$ starts to decrease at $T_{ed} \sim 6$ eV. This behaiour is considered to result from a lack of ionization caused by the low electron temperature.

Ionization rates in the divertor are calculated from $n_{ed}$, $T_{ed}$, neutral gas density /2/ and ionization cross-sections /13,14/[+]. The following assumptions are made for ohmic D-operation:

1. the neutral gas density is constant,
2. the pressure $n_{ed} \cdot T_{ed}$ is constant along magnetic field lines, and
3. the energy flow along magnetic field lines is carried only by electron heat conduction.

The first assumption is justified across the scrape-off layer, where the ionization probability is much less than 1 (e.g. $\lesssim 0.2$), but is not correct near the divertor throat where the ionization probability is rather high. The other assumptions are reasonable. The calculated result is consistent with the total particle loss obtained from the measured ion saturation currrent and is shown in Fig. 11 for D-operation with ohmic heating. Production rates of $D^+$ in the divertor ($S_d$ near the divertor plate, $S_{th}$ near the divertor throat) are shown by dotted lines. The average production rate of $D^+$ in the divertor $\bar{S}$ is shown by a solid line. The calculated electron temperature $T_{eth}$ at the throat, and the measured $n_{ed}$ and $T_{ed}$ near the divertor plate are also shown in the same figure. The average or total production rate of $D^+$, $\bar{S}$, increases when $\bar{n}_e$ is raised from $1 \times 10^{13}$ $cm^{-3}$ to $5 \times 10^{13}$ $cm^{-3}$ and the divertor plasma suppresses strong neutral gas back flow into the main plasma. With a higher density in the main plasma, i.e. $\bar{n}_e > 4.5 \times 10^{13}$ $cm^{-3}$, or a lower electron temperature in the divertor, i.e. $T_{ed} < 6$ eV or $T_{eth} < 12$ eV, the production rate saturates or decreases with increasing $\bar{n}_e$. The neutral gas density in the divertor, however, increases steeply /2/ and strong gas back flow into the main chamber is no longer suppressed resulting in a sudden disruption.

---

[+] In this calculation, ionization only from $D_2$ is assumed and ionization from $D^o$ reflected from the neutralizer plate is neglected. Thus the calculated production rate of $D^+$ gives a lower value.

The observed results show that the minimum electron temperture in the divertor is determined by the disruption condition. The maximum density is the value which corresponds with the minimum temperature. The divertor plasma is maintained by energy flow from the main plasma. Therefore the maximum density has to be a strong function of power flow into the divertor. The major part of the heating power flows into the divertor, and the relation between the heating power and the observed maximum density is shown in Fig. 12. The maximum density is proportional to the input power as expected.

In ASDEX, the minimum electron temperature near the neutralizer plate is around 5 eV in a stable discharge and the concept of a gas neutralizer is not realized.

## 6. Discussions

A strong inhomogeneity along magnetic field lines was expected from the recent numerical study by W. Schneider and K. Lackner /7/ and was demonstrated in section 3. This inhomogeneity is stronger with neutral beam injection because of the high heat flux, and is considered to be caused mainly by the finite electron conductivity along magnetic field lines. Calculated electron temperatures at the torus mid-plane are compared with the measured data in Table 1. In this calcualtion, the energy flow only due to the electron heat conduction along the magnetic field lines is considered.

| | (1) NBI | | (2) OH | | (3) NBI | | (4) OH | |
|---|---|---|---|---|---|---|---|---|
| $I_p$ | 380 kA | | 380 kA | | 200 kA | | 200 kA | |
| $\bar{n}_e$ | $8\times10^{13}cm^{-3}$ | | $1.5\times10^{13}cm^{-3}$ | | $3.5\times10^{13}cm^{-3}$ | | $1.8\times10^{13}cm^{-3}$ | |
| | $n_e$ | $T_e$ | $n_e$ | $T_e$ | $n_e$ | $T_e$ | $n_e$ | $T_e$ |
| Torus Mid-plane | 8 | 90 (75) | 1.5 | 55 (45) | 4 | 90 (90) | 1 | 40 (40) |
| Divertor Region | 100 | 10 | 4.5 | 20 | 25 | 15 | 2.5 | 15 |

TABLE 1: Densities $n_e$ ($10^{12}cm^{-3}$) and electron temperatures $T_e$(eV) at the separatrix measured in the torus mid-plane and in the divertor region, respectively, for different discharge conditions. Profiles are shown in Fig. 4 and 5. Calculated temperatures at the torus mid-plane are shown in brackets.

These calculated values seem reasonable, so that the dominant proces in the heat flow can be consdiered to be the electron heat conduction along the magnetic field lines. On the surface of the divertor plate, however, the heat flux is carried through the sheath and the power flow P onto the divertor plate is given by the following simple formula from the sheath theory as demonstrated in DIVA /15/:

$$P = \int \gamma \, i T_e \, dS. \qquad (2)$$

Here $\gamma$, i and $T_e$ are heat conductiion rate, ion saturation current density ($A/cm^2$) and electron temperature near the sheath (eV). The heat conduction rate is expected to be around 7 - 10 in this experiment if we assume $T_e = T_i$. Values $i_s$ and $T_{ed}$ are measured near the divertor plate (Fig. 1) and $i \sim i_s$ and $T_e \sim T_{ed}$. Therefore the total power can be calculated from the measured $T_{ed}$ and $i_s$ and is shown in Fig. 13. In this calculation we assume up-down symmetry with 20 % power loss onto the inner plate and 80 % onto the outer plate. The calculated total power loss is around 150 kW or 50 % of the input power with $T_{ed} \gtrsim 10$ eV or $\bar{n}_{ed} \lesssim 10^{13}$ $cm^{-3}$ in ohmic discharge and is reduced by a large factor with decreasing $T_{ed}$ or increasing $n_{ed}$. This value seems low but is within experimental uncertainties. The strong reduction of the heat flux with low $T_{ed}$ (<10 eV) or high $n_{ed}$ (>$10^{13}$ $cm^{-3}$) is considered to result from a large radiation and charge exchange loss in the divertor /16/. With neutral beam heating, the situation is more complex. With $T_{ed}$ < 15 eV or with $n_{ed}$ > 3 x $10^{13}$ $cm^{-3}$, the situation is similar to that without neutral beam injection. With a high $T_{ed}$ or a low $n_{ed}$, the calculated power loss is very small, e.g. 0.3 MW with $P_{NI}$ = 2.5 MW. In H-type discharges /4/, the calculated heat loss onto the divertor plate is also small, e.g. 0.3 MW, even with a rather low temperature as shown by (◇) in Fig. 13. These small values for the calculated power loss onto the divertor plate are not understood. But some possible explanations are discussed below.

In Fig. 14, equipartition time $\tau_{eq}$ and particle life time (or particle recycling time) $\tau_{pdiv}$ in the divertor are shown for the ohmic D-operation as a function of the main plasma density. In the high density, $\tau_{eq} < \tau_{pdiv}$ and it is reasonable to assume $T_i = T_e$. But for low density ($n_{ed} < 5 \times 10^{12}$ cm$^{-3}$ and $T_{ed} > 15$ eV) $\tau_{eq} > \tau_{pdiv}$. It is not reasonable to assume $T_i = T_e$ in the high $T_{ed}$ case, especially with neutral beam injection. This effect has a possibility to increase the power loss onto the divertor plate and/or to increase the cx loss at a low $n_{ed}$ or a high $T_{ed}$. $\tau_{pdiv}$ is defined by

$$\tau_{pdiv} = N_{ed}/F_w, \tag{3}$$

where $N_{ed}$ is the total electron number in the scrape-off layer and $F_w$ is the total particle source flux S or the total particle loss flux.

Another uncertainty may come from observed large fluctuations of the divertor plasma during the heating phase as shown in Figs. 15 and 16. Large spontaneous particle losses are observed especially in an H-type discharge. The electron temperature of this spontaneous loss flux is estimated to be higher than the normal value, e.g. $T_e > 30$ eV for the spontaneous loss flux with a normal temperature of 10 eV, and a large heat flux may be carried by these spontaneous losses. These spontaneous losses correlate with sawteeth like fluctuations of the main plasma density as shown in Fig. 16 (2). The time delay between the denstiy drop in the main plasma and the spontaneous particle flux is very short, i.e. less than 1 ms, and this type of loss is not observed with a normal sawtooth oscillation. Therefore this spontaneous loss may be induced by a density drop in the periphery plasma. The heat flux carried by these losses have not been investigated but cannot be neglected.

The mean density in the divertor is considered to be a strong function of the mean plasma density in the main chamber /1,9/ but has been shown to be strongly affected by the recycling condition (section 4). Therefore no simple relation between $n_{ed}$ and $\bar{n}_e$ can be observed under various discharge conditions, as shown in Fig. 17 because of the strong inhomogeneity along magnetic field lines as shown in section 3 and the divertor plasma can change without changing the main plasma as shown in section 4. In Fig. 18, $n_{ed}$ and $T_{ed}$ are plotted, and a strong relation can be observed between them for a constant heating power. This result suggests that the essential relation between the divertor plasma and the main plasma is only through the power flow. The power flow into the divertor maintains the divertor plasma. Other parameters can change within a wide range, e.g. $n_{ed}$ can be changed by increasing the particle source in the divertor and the particle source can be controlled not only by the main plasma but also by the divertor condition as shown in section 4. This characteristic of the divertor plasma is very important for controlling the divertor plasma for a given main plasma. For example the electron temperature near the divertor plate is kept at a low value by controlling the neutral gas source in the divertor where the mean density in the main chamber is kept constant with $P_{NI}$ = 0.3 - 2.5 MW. The observed low electron temperature, $T_{ed}$ = 7 eV, at a high density, $n_{ed} = (1 \sim 1.7) \times 10^{13}$ cm$^{-3}$ with OH and $n_{ed} = (0.8 \sim 1.5) \times 10^{14}$ cm$^{-3}$ with $P_{NI}$ = 2.5 MW, can be explained by eq. (1) with a small value of $\bar{\tau}_p/\tau_E$ and a rather large value of $P_r$. If $\tau_E = 1.0 \times 10^{-15} \cdot \bar{n}_e$ sec in the main plasma with OH, $\bar{\tau}_p/\tau_E \sim 0.1$ at $\bar{n}_e = 5 \times 10^{13}$ in D-operation. Equation (1) gives $T_{ed} \sim 0.04\ \bar{T} \times (P_{in} - P_r)/P_{in}$ and a rather large $P_r$, $P_r/P_{in} \sim 0.8$ /15/, gives a reasonable value for $T_{ed}$. The calculated over-all particle confinement time $\bar{\tau}_p$ for OH plasmas is shown in Fig. 19. $\bar{\tau}_p$ is defined by

$$\bar{\tau}_p = N_e/F_w, \qquad (4)$$

where $N_e$ and $F_w$ are the total number of electrons and the total loss flux onto the first wall, respectively. Since almost all particles lost from the main plasma flow into the divertor, the total flux can be calculated by

$$F_w = \frac{1}{e} \int i_s \, dS, \tag{5}$$

where $i_s$ is the ion saturation current measured near the divertor plate. The figure shows an increase in $\bar{\tau}_p$ with increasing $\bar{n}_e$ up to 2 x $10^{13}$ $m^{-3}$ and a decrease in $\bar{\tau}_p$ with increasing $\bar{n}_e$ from 3 x $10^{13}$ $cm^{-3}$. This characteristic shows that $\bar{\tau}_p \sim \tau_p$ in a low density discharge because of small ionization in the divertor chamber. $\tau_p$ is the particle confnement in the main plasma and defined by

$$\tau_p = N_{em}/F_D, \tag{6}$$

where $N_{em}$ is the total electron number in the main plasma and $F_D$ is the net particle loss into the divertor or the total net particle source in the main chamber. The expected $\tau_p$ is shown by a dotted line in Fig. 19. In a high density discharge, ionization in the divertor becomes dominant, and $\bar{\tau}_p \ll \tau_p$ as shown. With neutral beam heating, a very high density is obtained in the divertor and a very small value for $\bar{\tau}_p$ is obtained as shown in Fig. 20. $\bar{\tau}_p/\tau_E \sim 0.03$ for a high density discharge. This equation is consistent with the measured value of $T_{ed}$. This same situation can be realized with a rather low density discharge by puffing gas into the divertor as shown in section 4. This result is very encouraging to future large experiments with poloidal magnetic limiters, such as JT-60, ASDEX-Upgrade and INTOR designed in the phase O.

In ASDEX, the minimum electron temperature near the divertor plate is around 5 ~ 6 eV in a stable discharge because of the strong gas back flow into the main chamber and the induced

disruptions which result. The gas neutralizer is not realized. In order to realize the gas neutralizer, a much lower temperature has to be obtained by reducing the gas back flow. A possibility for reducing the gas back flow is by elongating the divertor plasma layer, or by reducing the divertor throat width. The throat width was reduced from 5.5 cm to 3.3 cm but no significant change was observed as shown in Fig. 21. Therefore it is concluded that a much deeper and narrower divertor is required for the gas neutralizer; and this kind of divertor cannot be applied to a reactor because of the resulting complexity.

It is very interesting to compare the experimental results with the numerical results /7/. Good agreements are observed in the following points:

1. Divertor density variation with main plasma density exhibits three regions, i.e. small change at low densities in the main chamber, a steep change at medium densities and a saturation at high density.

2. The maximum density in the divertor is proportional to the heating power.

3. A strong inhomogeneity along the plasma flow with an intense heat flux.

These good agreements in the essential plasma characteristics support the numerical model employed in ref. /7/. For low divertor plasma density we cannot find a good agreement and cannot understand the results. For a more detailed comparison between numerical and experimental results it is important to measure changes in plasma parameters along the magnetic field lines in the divertor as well as to measure ion temperature and power balance in the divertor.

## 7. Summary

Characteristics of divertor plasma with neutral beam injection ($P_{NI} \leq 2.5$ MW) are studied with the following conclusions:

1. A strong inhomogeneity along magnetic field lines in a scrape-off layer is obtained especially with high power heating, e.g. $T_{eb} \sim 100$ eV and $n_{eb} \sim 10^{13}$ cm$^{-3}$ at the torus mid-plane in the main chamber and $T_{ed} \sim 10$ eV and $n_{ed} \sim 10^{14}$ cm$^{-3}$ near the divertor plate. This is mainly due to finite electron conductivity along magnetic field lines as expected from numerical studies /7/.

2. Plasma parameters near the divertor plate such as $T_{ed}$ and $n_{ed}$ are strong functions of recycling conditions in the divertor, e.g. gas source, pump and width of the divertor throat, as well as discharge conditions in the main chamber, e.g. density, heating power and confinement. Therefore, there is no simple relation between the divertor plasma parameters and the main plasma parameters such as $n_{ed} = f(\bar{n}_e)$. The divertor plasma is mainly affected by the power flow from the main plasma.

3. The electron temperature $T_{ed}$ is a strong function of the electron density $n_{ed}$ and the heating power, i.e. $T_{ed}$ decreases with increasing $n_{ed}$ and with reduction in heating power.

4. An ideal divertor plasma with a low temperature and a high density is obtained in a stable discharge even with neutral beam injection. For example, $T_{ed}$ is maintained at a low value of 7 eV by increasing $n_{ed}$ from $10^{13}$ cm$^{-3}$ to $1.2 \times 10^{14}$ cm$^{-3}$ when the heating power increases from 0.35 MW to 2.5 MW with a constant value of the main plasma density of $7 \times 10^{13}$ cm$^{-3}$. This situation is realized by increasing recycling in the divertor (or reducing the over-all particle life time). The over-all particle confinement time $\bar{\tau}_p$ is reduced to 0.5 - 1 ms with neutral

beam heating. $\bar{\tau}_p = N_e/F_w$ where $N_e$ and $F_w$ are the total electron number and the total particle loss flux onto the wall surfaces.

5. The gas neutralizer was not obtained in ASDEX for the following reason. At a very low value of $T_{ed}$, the ionization coefficients of hydrogen are very small, the divertor plasma cannot stop a strong neutral gas back flow from the divertor chamber and disruptions are induced. Thus, the the minimum electron temperature is around 5 eV in a stable discharge. A plamsa with a much lower temperature is required for the gas neutralizer. Therefore, a deeper and narrower divertor is required to realize the gas neutralizer and is not realistic in a future large device because of its complexity.

6. Observed characteristics of divertor plasma are consistent with numerical studies /7/ qualitatively. At a low density near the divertor plate, however, characteristics are not understood.

The result is encouraging to development of future large devices with a magnetic poloidal divertor such as JT-60, ASDEX-upgrade and INTOR.

ACKNOWLEDGEMENTS

The authors thank our colleagues from the ASDEX group, particularly Drs. H. Niedermeyer and E.R. Müller for fruitful discussions and also Dr. Yip Hoi Tung for his help to calculate production rate of $D^+$.

## Appendix

Absolute plasma density from Langmuir probe measurement is obtained by calibrating the probe signal with 3.3 mm μ-wave cut-off density. Geometrical relations between two diagnostics are shown in Fig. 1. The calibrated point is denoted by (●) in Fig. 22. Line densities from the probe measurement are compared with those from the μ-wave interferometer in the same figure. The accuracy is rather good as shown in the figure but the probes have to be carefully treated because they are easily damaged due to a large heat deposition (a few hundreds $W/cm^2$ with OH and a few $kW/cm^2$ with $P_{NI}$ = 2.5 MW).

When using probes, it has to be carefully discussed whether the probe affects or changes the plasma. The probe located near the neutralizer plate is much smaller than the neutralizer plate and is considered not to affect the divertor plasma. In the experiment, three sets of probes are tested at the same time and give the same profiles. This result shows that the probes do not affect the divertor plasma strongly.

In this paper, peak values of electron temperature and density profiles are mainly discussed. The peak position of a profile moves with changing discharge conditions as shown in Fig. 23. This is mainly due to change of the magnetic configuration. The most important parameters are $I_v/I_p$ and $I_M/I_p$ where $I_v$, $I_p$ and $I_M$ are vertical coil current, plasma current and multipole coil current. In Fig. 23, the measured peak positions ($d_p$) are shown with various values of $I_v/I_p$ and with a constant value of $I_M/I_p$. In Fig. 24, the peak position is shown for two values of $I_M/I_p$ with a constant value of $I_v/I_p$. The peak position is not located exactly at the separatrix magnetic surface. This may be due to ExB drift effects. In Fig. 25, peak positions are shown for H- and D-discharges and is the order of two poloidal Larmor radius. This effect is expected from ExB drift due to a pre-sheath potential gradient of around $T_e$.

The other improtant magnetic parameters of a divertor configuration are summarized in Fig. 26.

References

/1/ KEILHACKER, M. et al., "Impurity control experiments in the ASDEX divertor tokamak", Proc. 8th Int. Conf. on Plasma Physics and Contr. Nucl. Fusion Research, Brussels 1980, Vol. II, IAEA, Vienna (1981) 351.

/2/ KEILHACKER, M. et al., "Divertor operation at large power flows in neutral beam heated ASDEX discharges", 9th Int. Conf. on Plasma Phys. and Contr. Nucl. Fusion Research, Baltimore 1982, paper IAEA-CN-41/R-2.

/3/ DIVA-Group, Nucl. Fusion 18 (1978) 1619.

/4/ WAGNER, F. et al., "Confinement and $\beta_p$-studies in neutral beam heated ASDEX plasmas", 9th Int. Conf. on Plasma Phys. and Contr. Nucl. Fusion Research, Baltimore 1982, paper IAEA-CN-41/A-3.

/5/ SHIMOMURA, Y. "Some consideration of ash enrichment and ash exhaust by a simple divertor", Japan Atomic Energy Research Institute Report JAEARI-M 8294 (1979).

/6/ SHIMOMURA, Y., MAEDA, H., J. of Nucl. Materials 76 & 77 (1978) 45.

/7/ CHODURA, R. et al., "Self-consistent description of the plasma-wall interaction in tokamak plasmas", 9th Int. Conf. on Plasma Phys. and Contr. Nucl. Fusion Research, Baltimore 1982, paper IAEA-CN-41/D-3-1.

/8/ SHIMOMURA, Y., "A study on impurities and scrape-off layer plasma in a large tokamak", Japan Atomic Energy Research Institute Report JAEARI-M 7111 (1977).

/9/ SHIMADA, M. et al., "Heat load reduction of the divertor plate and formation of dense and cold divertor plasma by remote radiative cooling in Doublet-III and INTOR", Japan Atomic Energy Research Institute Report JAERI-M 9862 (1981).

/10/ NAGAMI, M. et al., "Divertor experiment in D-III", Proc. 8th Int. Conf. on Plasma Physics and Contr. Nucl. Fusion Research, Brussels 1980, Vol. II, IAEA, Vienna (1981) 367.

/11/ MAENO, M. et al., Nuclear Fusion 21 (1981) 1414.

/12/ MILLS, R.G., "A fusion power plant", Princeton Plasma Physics Laboratory Report, Matt-1050 (1974).

/13/ RAPP, H. et al., J. Chem. Phys. 42 (1965) 4081.

/14/ GROWE, J., McCONKEY, J.W., J. Phys. B6 (1973) 2088.

/15/ KIMURA, H. "Power balance in the divertor tokamak DIVA", Japan Atomic Energy Research Institute Report JAERI-M 8890.

/16/ KEILHACKER, M. et al., "Plasma boundary layer in limiter and divertor tokamaks", presented at 1982 International Conference on Plasma Physics, June 1982, Göteborg/Sweden; to be published in Physica Scripta.

/17/ GERNHARDT, J., private communication.

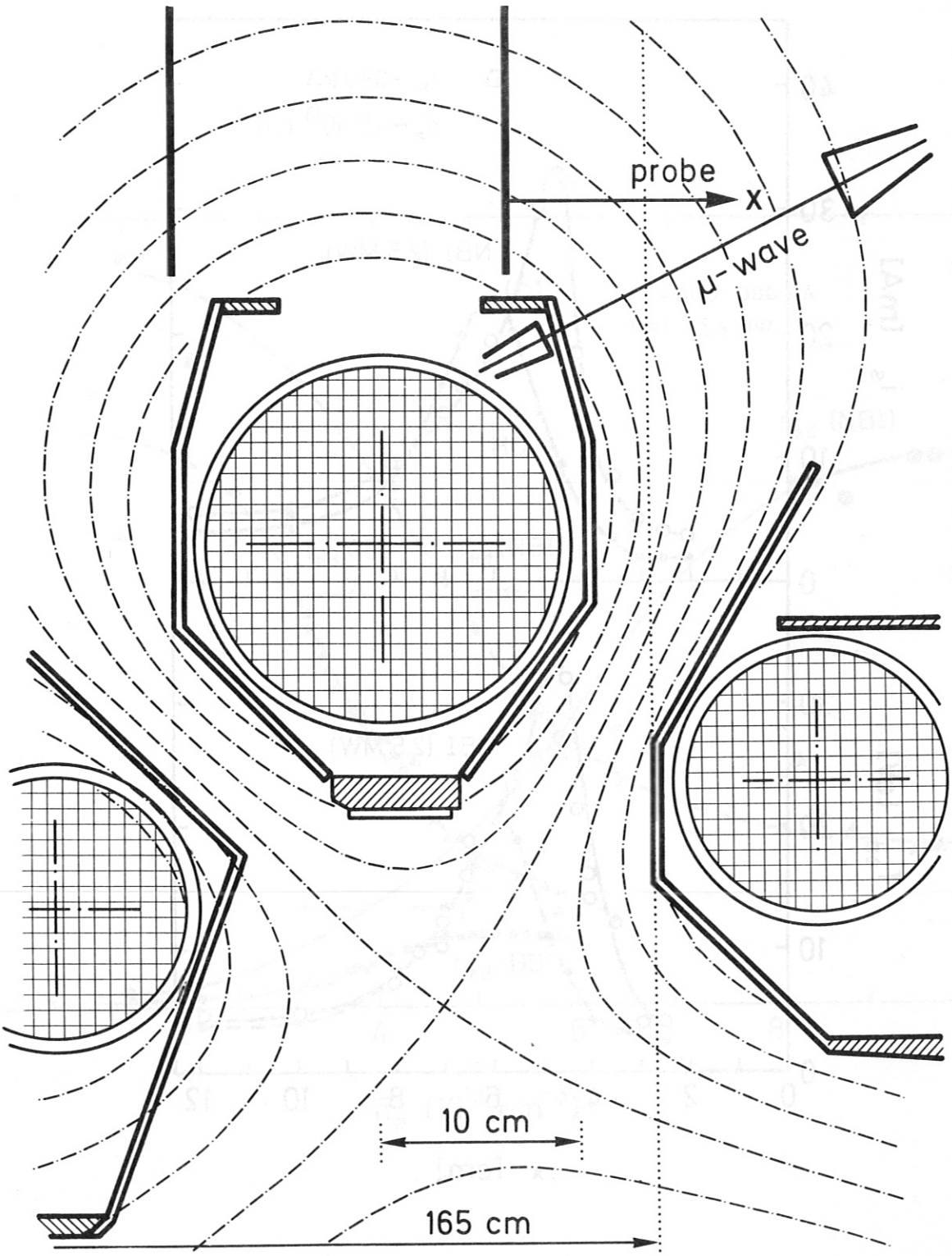


Fig.1: Schematic figure of ASDEX divertor indicating locations of probes and μ-wave hornes.

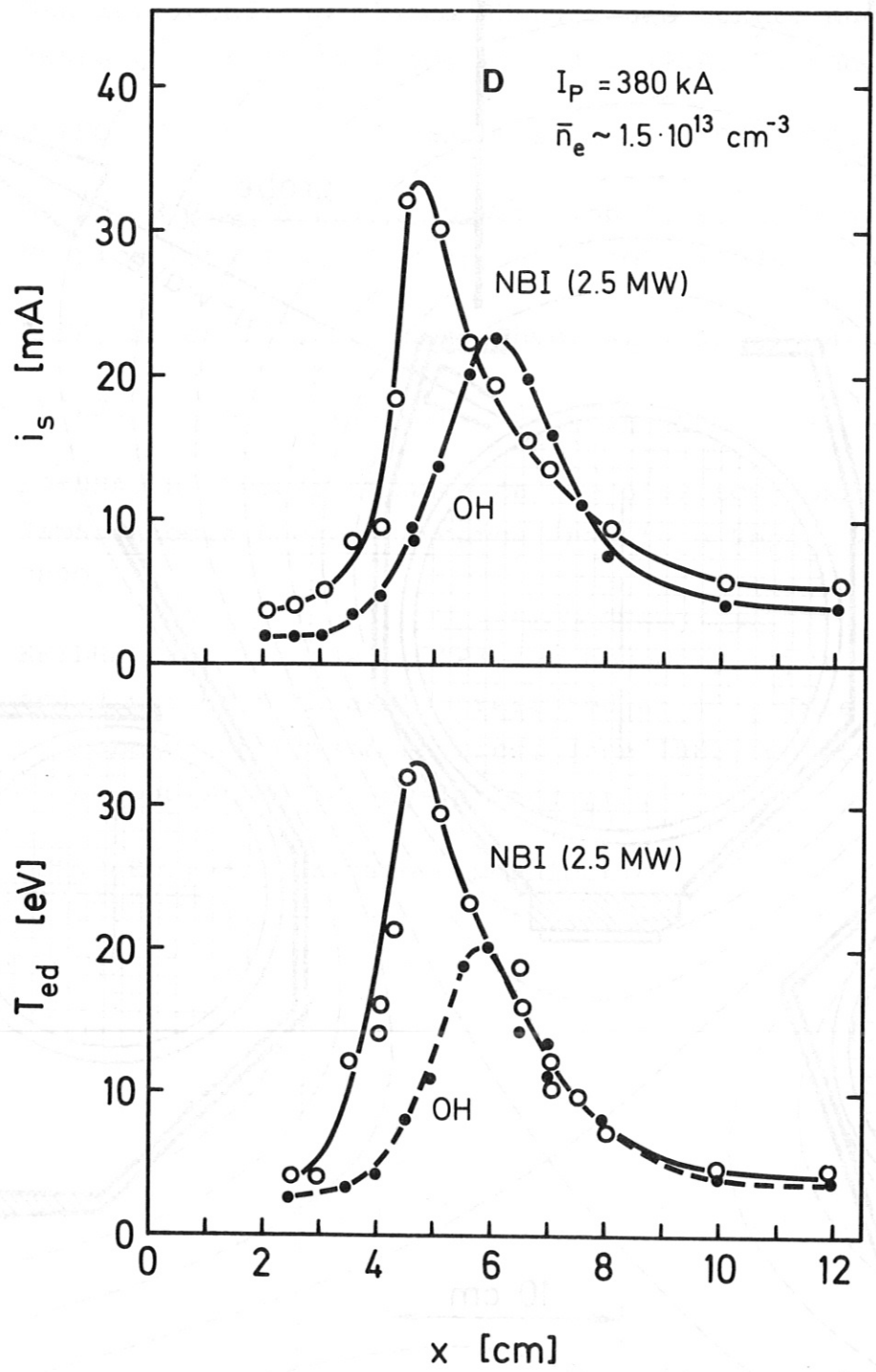


Fig.2: Profiles of the divertor plasma
$i_s$: Ion saturation current, $T_{ed}$: electron temperature; (•) without neutral beam injection and (O) with neutral beam injection.

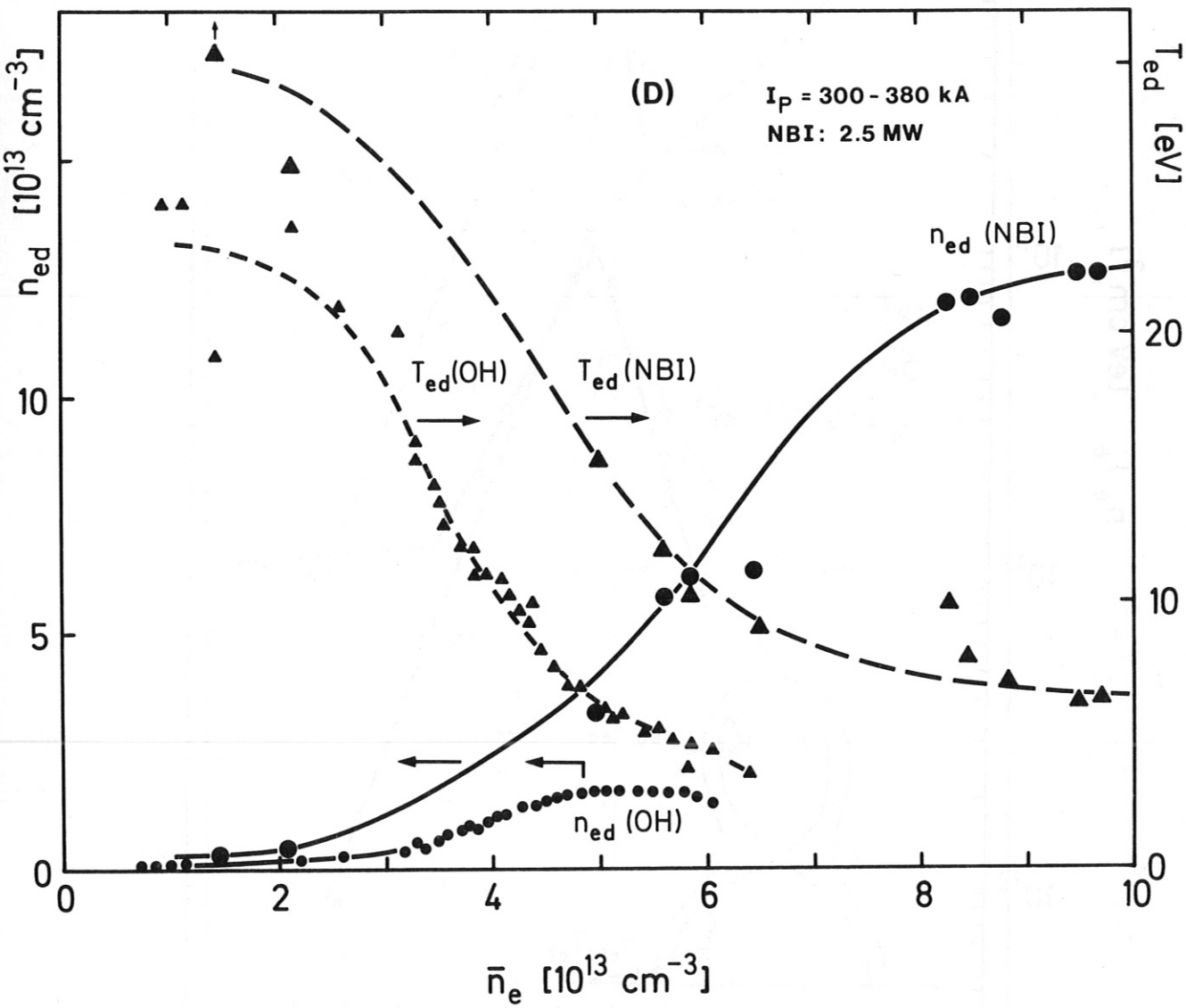


Fig.3: Peak values of electron temperature $T_{ed}$ (▲) and electron density $n_{ed}$ (●) near the divertor plate with and without neutral beam injection. Only the mean plasma density $\bar{n}_e$ in the main chamber is varied.

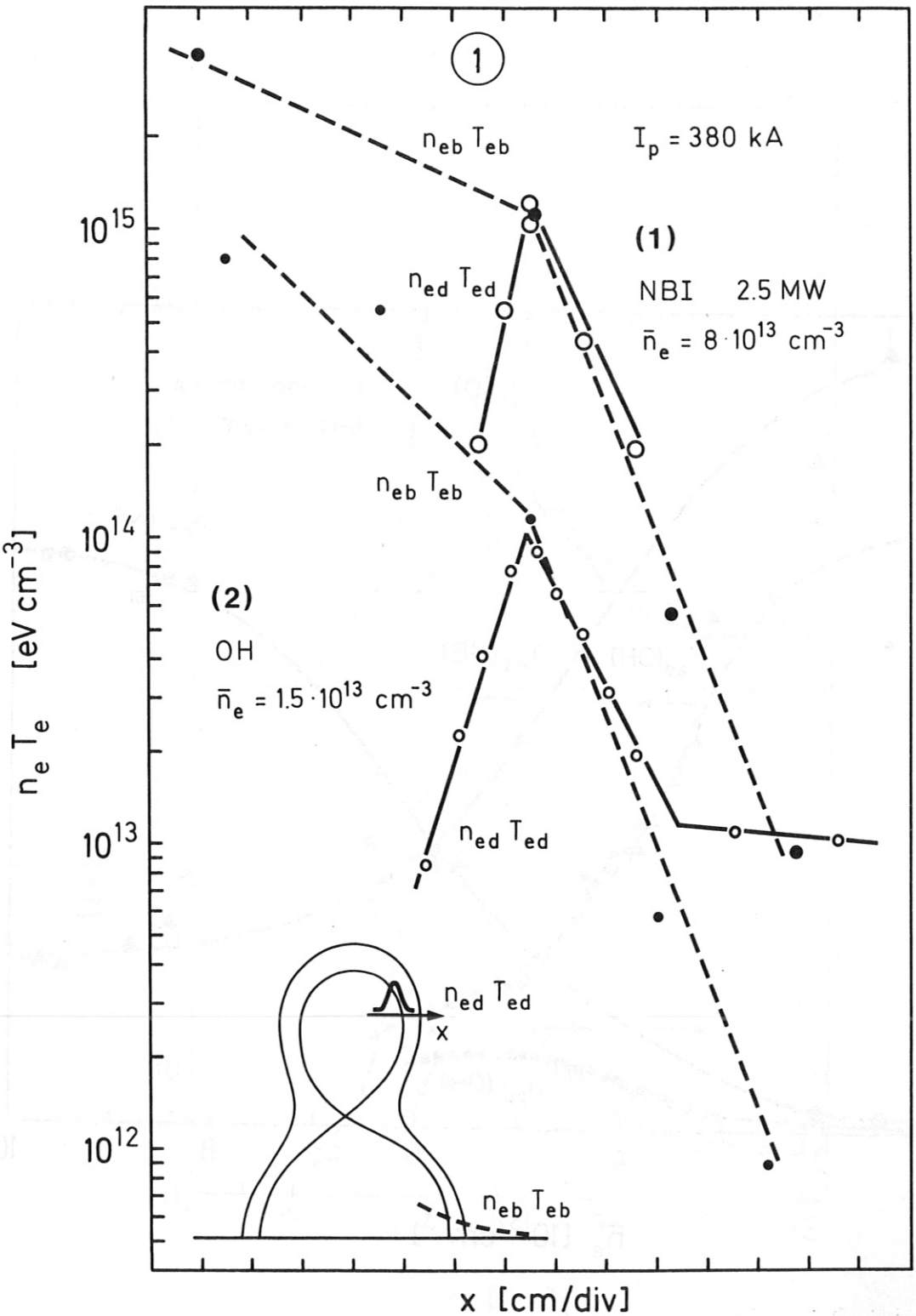


Fig.4,(1) and (2):
Measured electron pressure at the torus mid-plane ($n_{eb}T_{eb}$) and near the divertor plate ($n_{ed}T_{ed}$) for high current discharges with (1) and without (2) neutral beam injection. The horizontal axis shows the horizontal distance in the divertor. The horizontal distance at the torus mid-plane is around 2 cm/div.

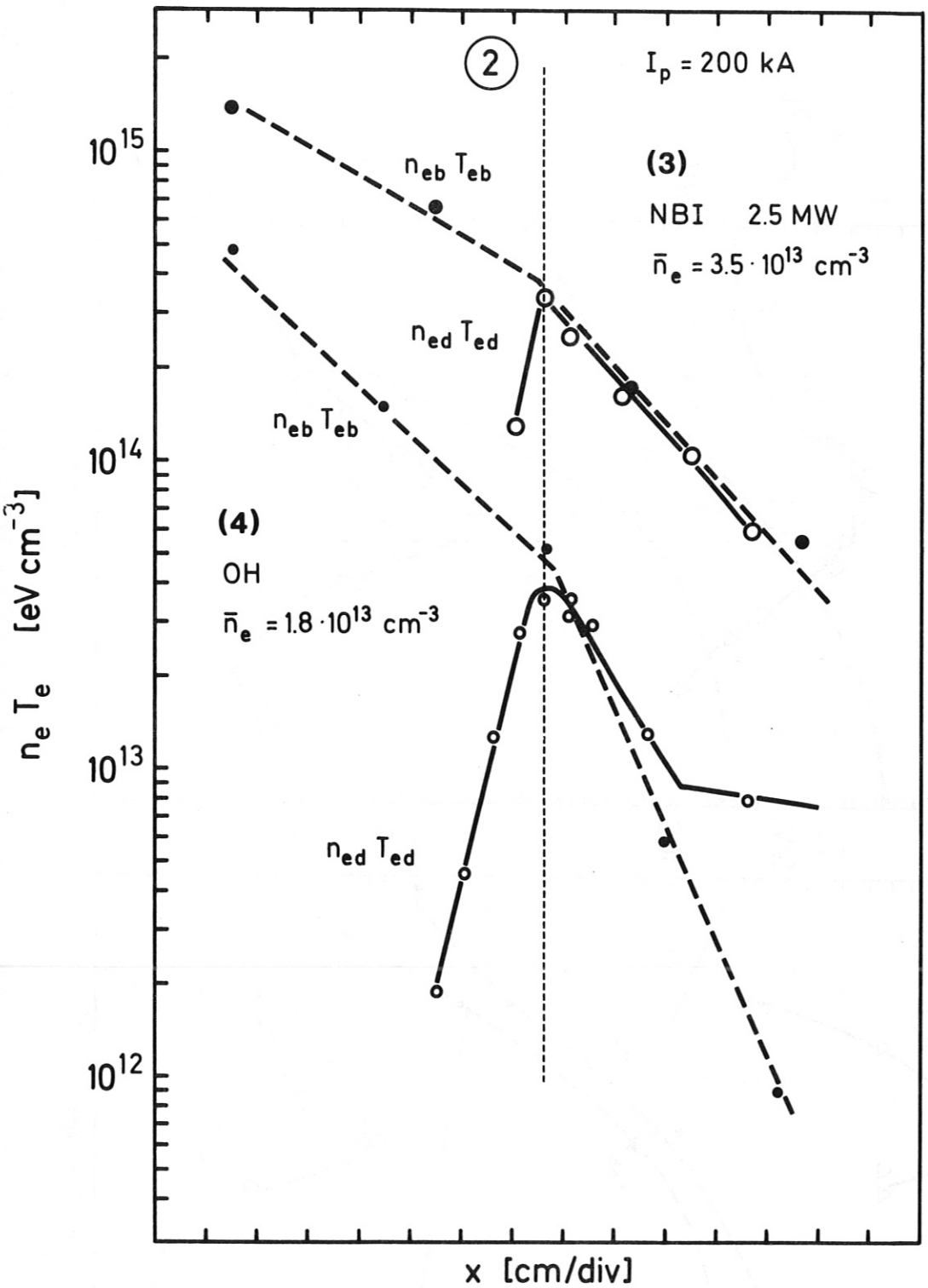


Fig.4, (3) and (4):
Measured electron pressure at the torus mid-plane ($n_{eb}T_{eb}$) and near the divertor plate ($n_{ed}T_{ed}$) for low current discharges with (3) and without (4) neutral beam injection. The horizontal axis shows the horizontal distance in the divertor. The horizontal distance at the torus mid-plane is around 2 cm/div.

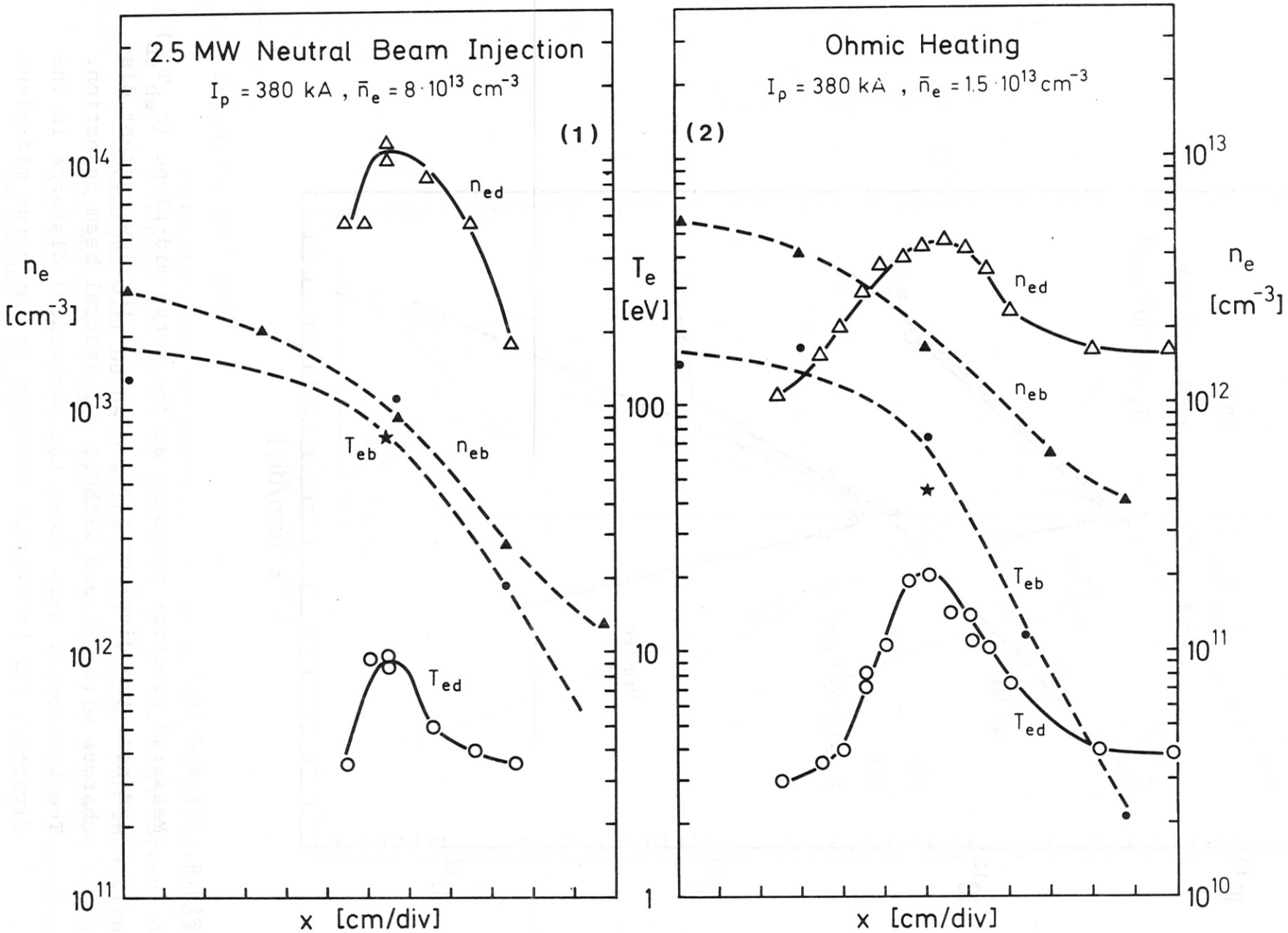


Fig.5, (1) and (2):
Profiles of electron density and temperature at the torus midplane ($n_{eb}$, $T_{eb}$) and near the divertor plate ($n_{ed}$, $T_{ed}$) for high current discharges with $P_{NI}$ = 2.5 MW (1) and ohmic heating (2), respectively. ★ calculated electron temperature.

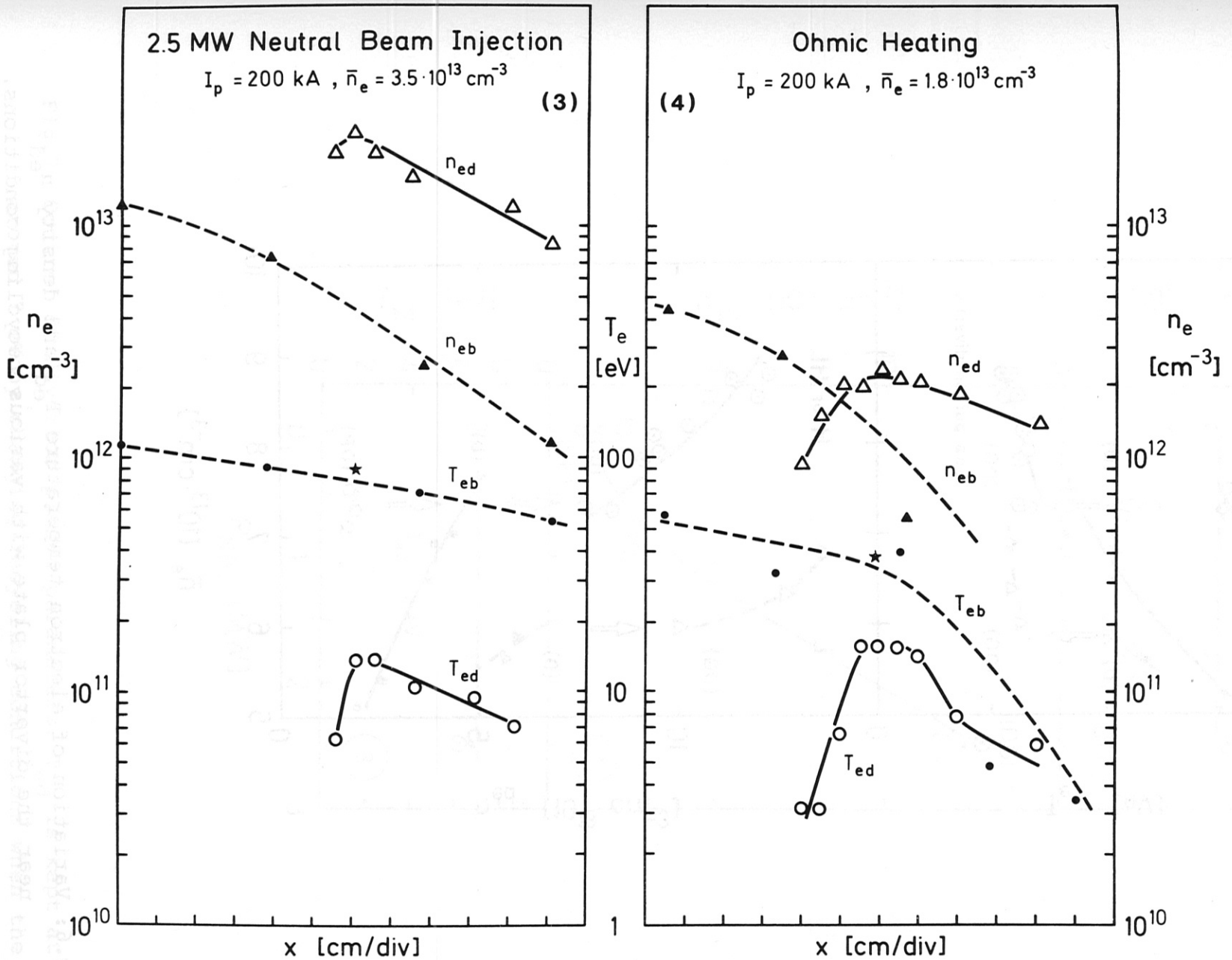


Fig.5, (3) and (4):
Profiles of electron density and temperature at the torus midplane ($n_{eb}$, $T_{eb}$) and near the divertor plate ($n_{ed}$, $T_{ed}$) for low current discharges with $P_{NI}$ = 2.5 MW (3) and ohmic heating (4), respectively. ★ calculated electron temperature.

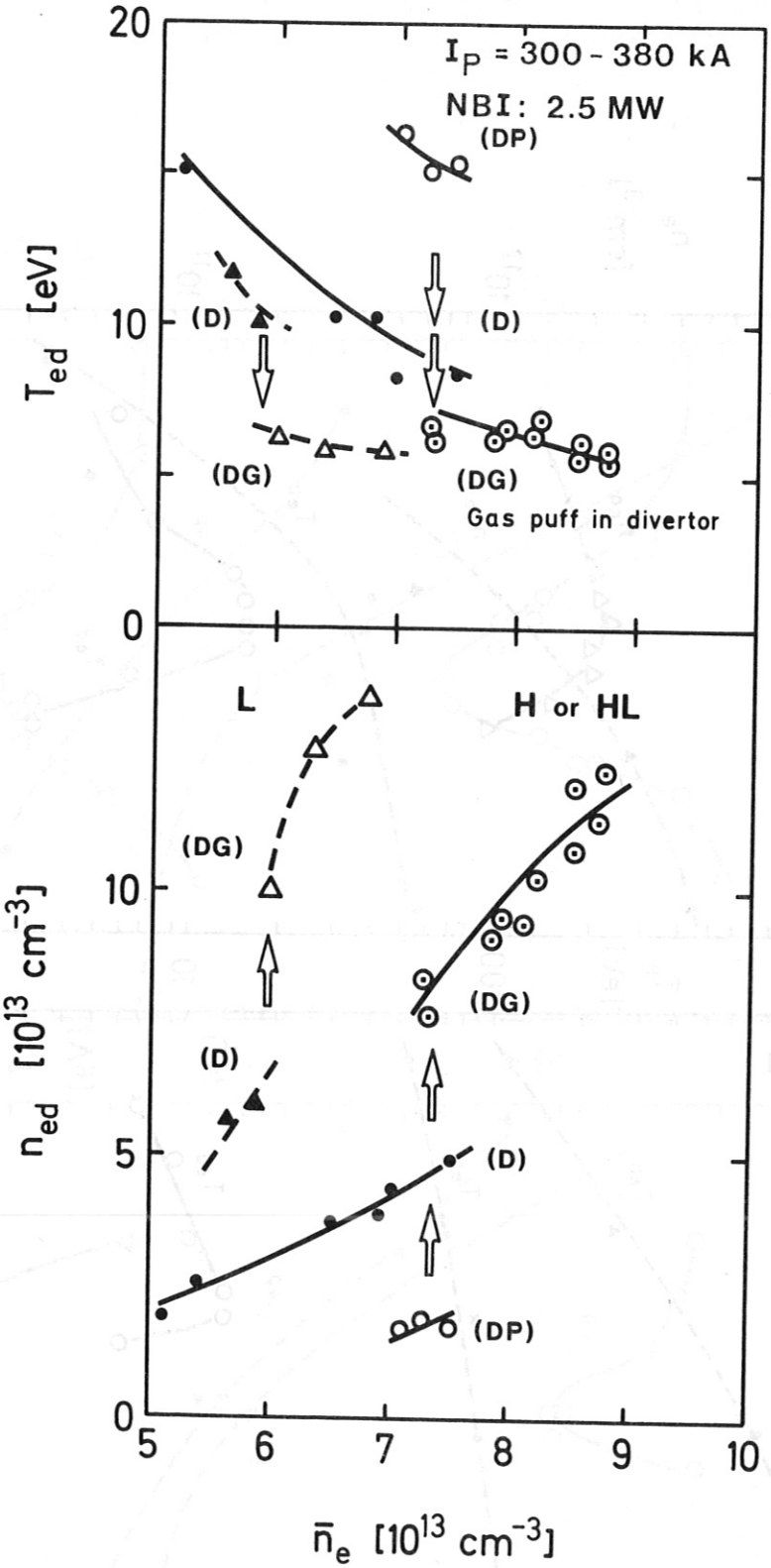


Fig.6: Variation of electron temperature $T_{ed}$ and density $n_{ed}$ near the divertor plate with various recycling conditions.
DP: pumping in diverotr
D: no pumping in divertor
DG: gas puffing in divertor
L and H denote L-type and H-type discharges /4/.

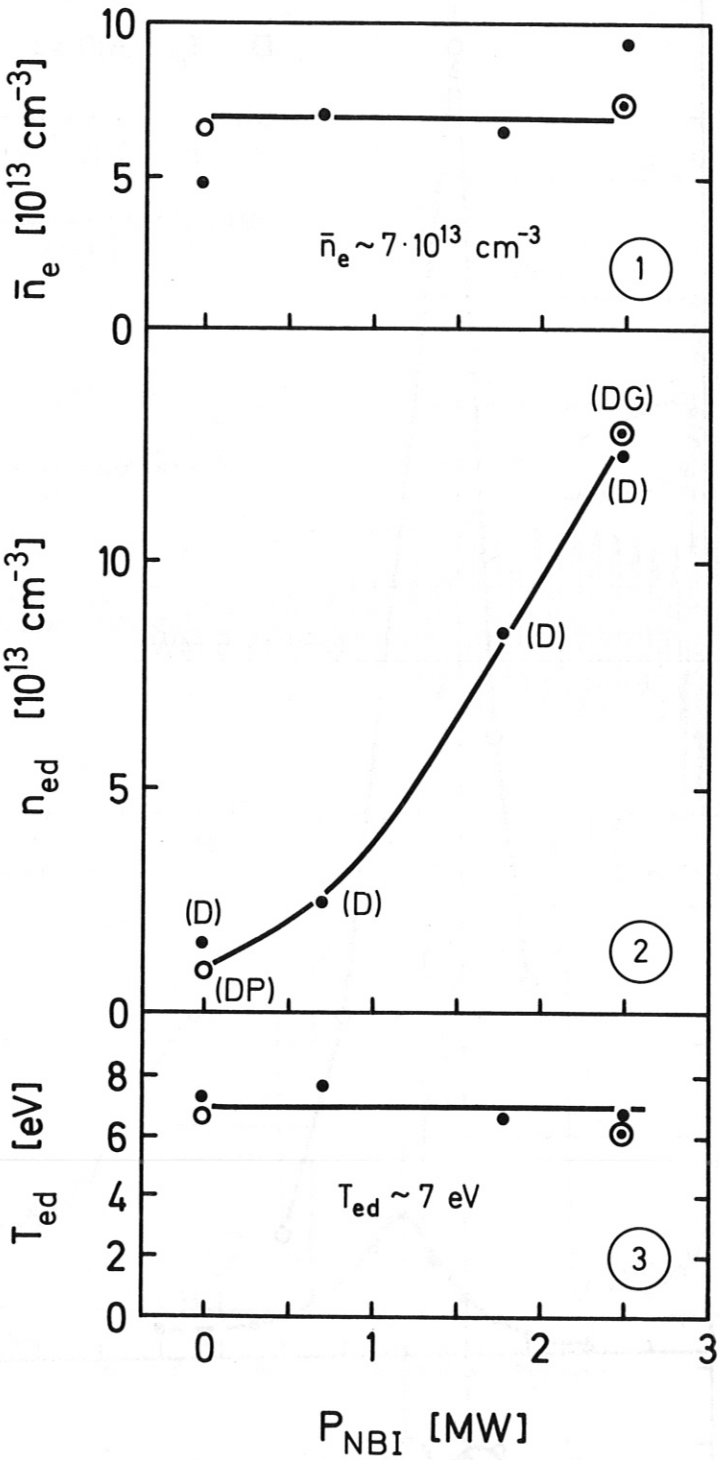


Fig.7: Control of divertor plasma parameters. $T_{ed}$ is kept at around 7 eV by changing recycling conditions when the neutral beam power $P_{NI}$ is raised from 0 to 2.5 MW.

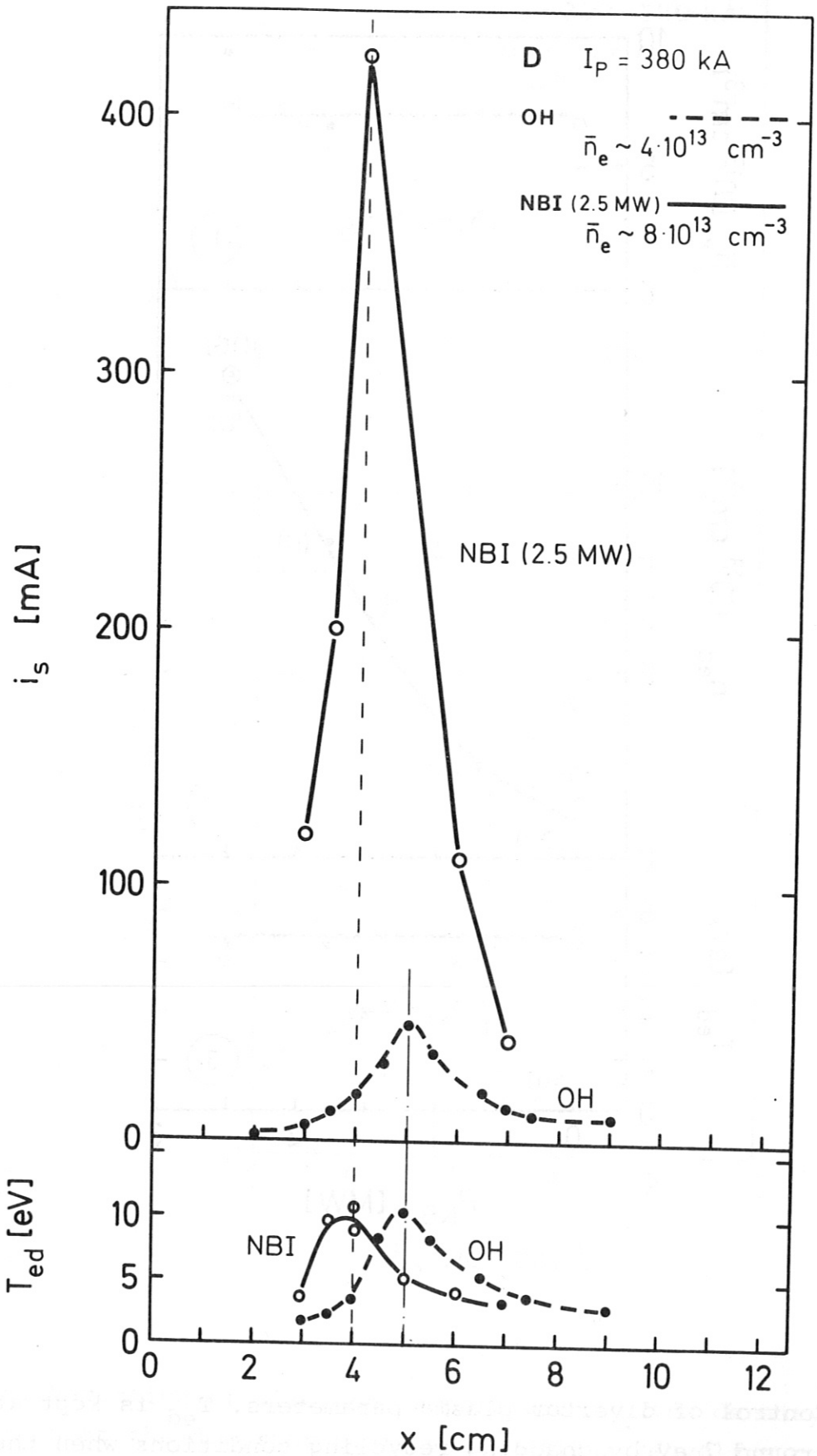


Fig. 8: Typical ion saturation current and electron temperature profiles with a low temperature $T_{ed}$.

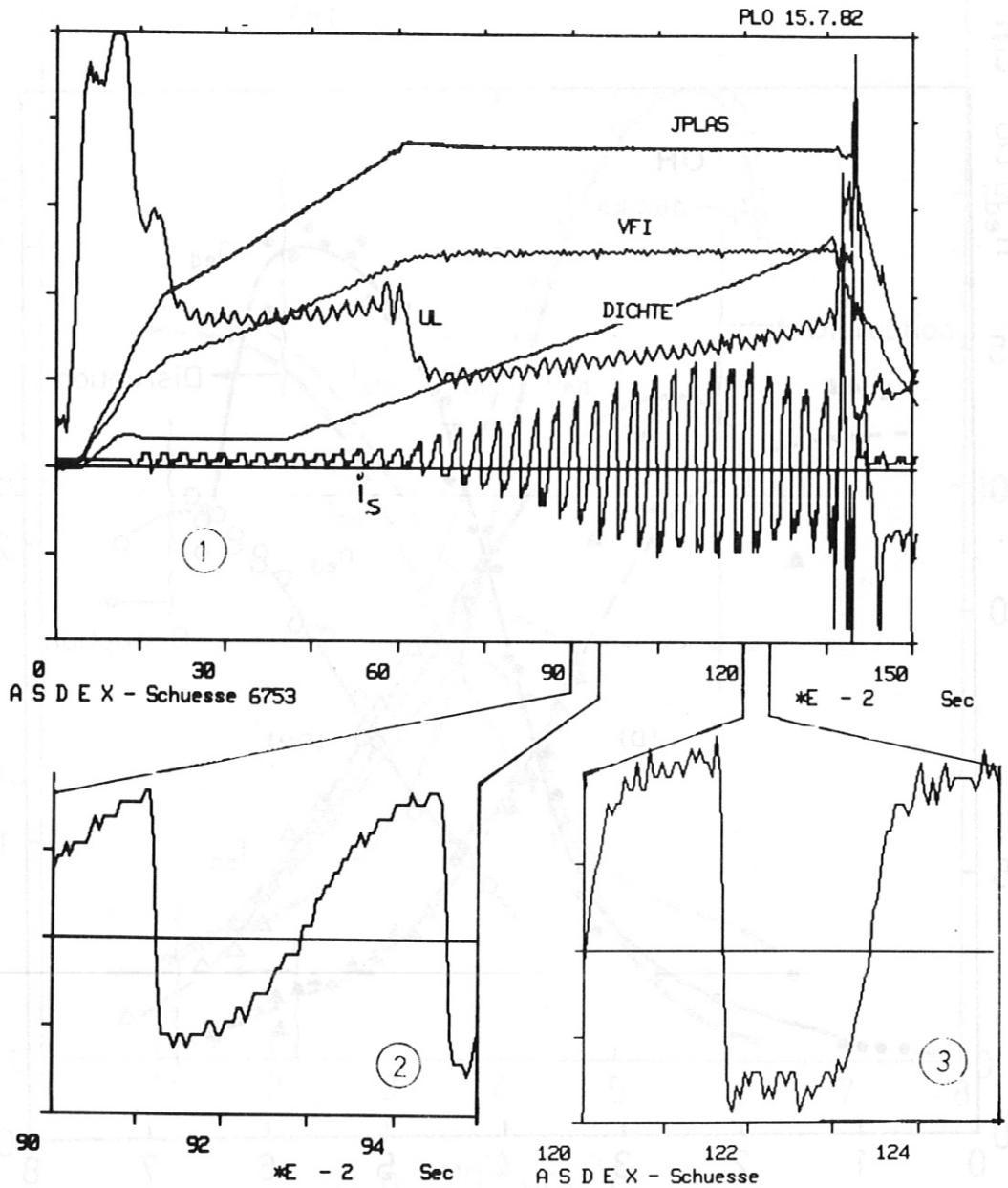


Fig.9: Disruption induced by intense gas puffing.
JPLAS: plasma current (100 kA/div.)
VFI: vertical field coil current (10 kA/div.)
DICHTE: mean electron density $\bar{n}_e$ ($2.8 \times 10^{13}$ $cm^{-3}$/div.)
UL: loop voltage (1 V/div.)
$i_s$: current of a double probe (sawteeth-like voltage is applied).
Detailed characteristics of $i_s$ are shown in (2) and (3) and a higher temperature is observed in (2).

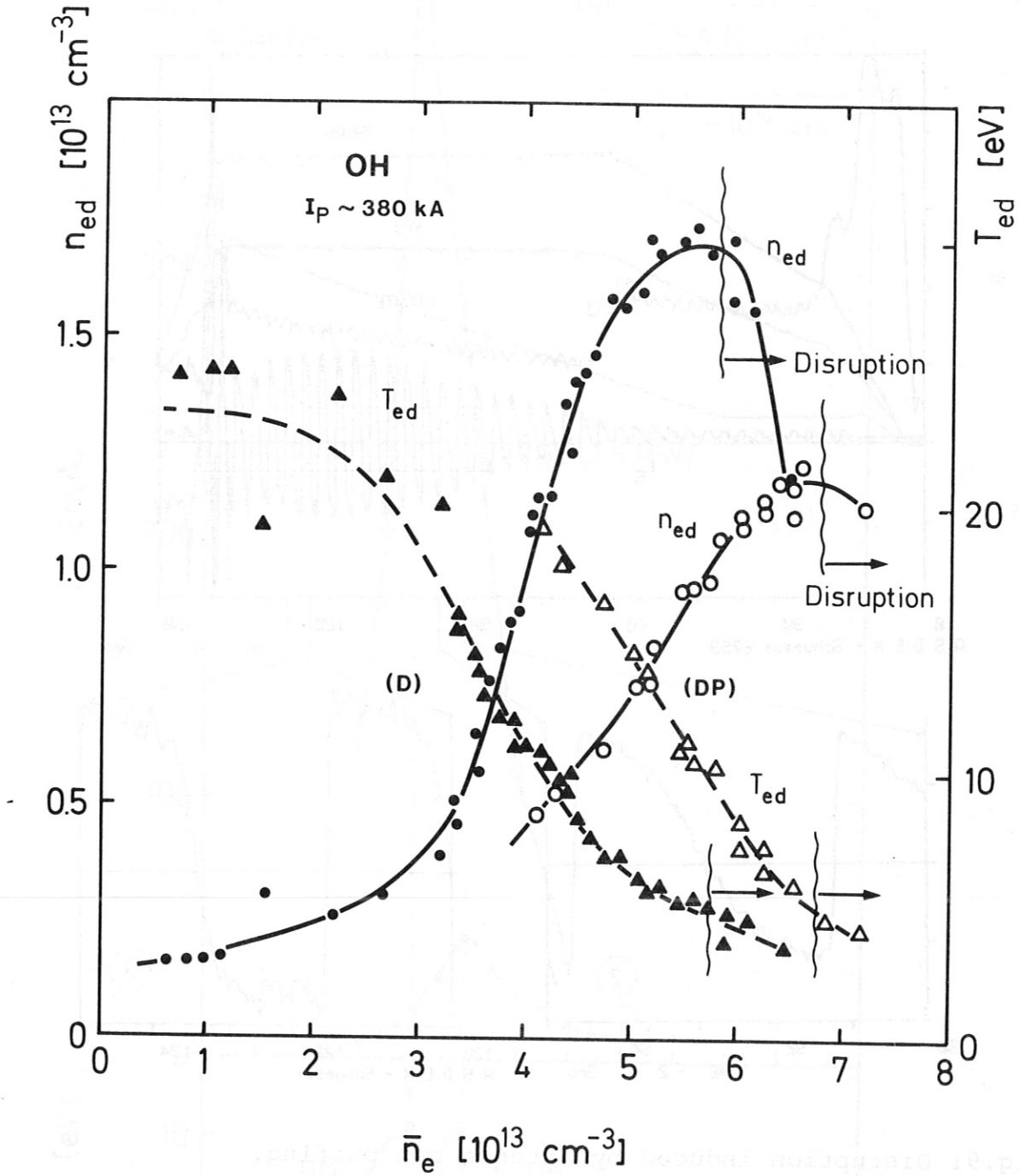


Fig.10: Minimum electron temperature $T_{ed}$. When $T_{ed} \lesssim 5$ eV, hard disruptions terminate the discharge for various discharge conditions.

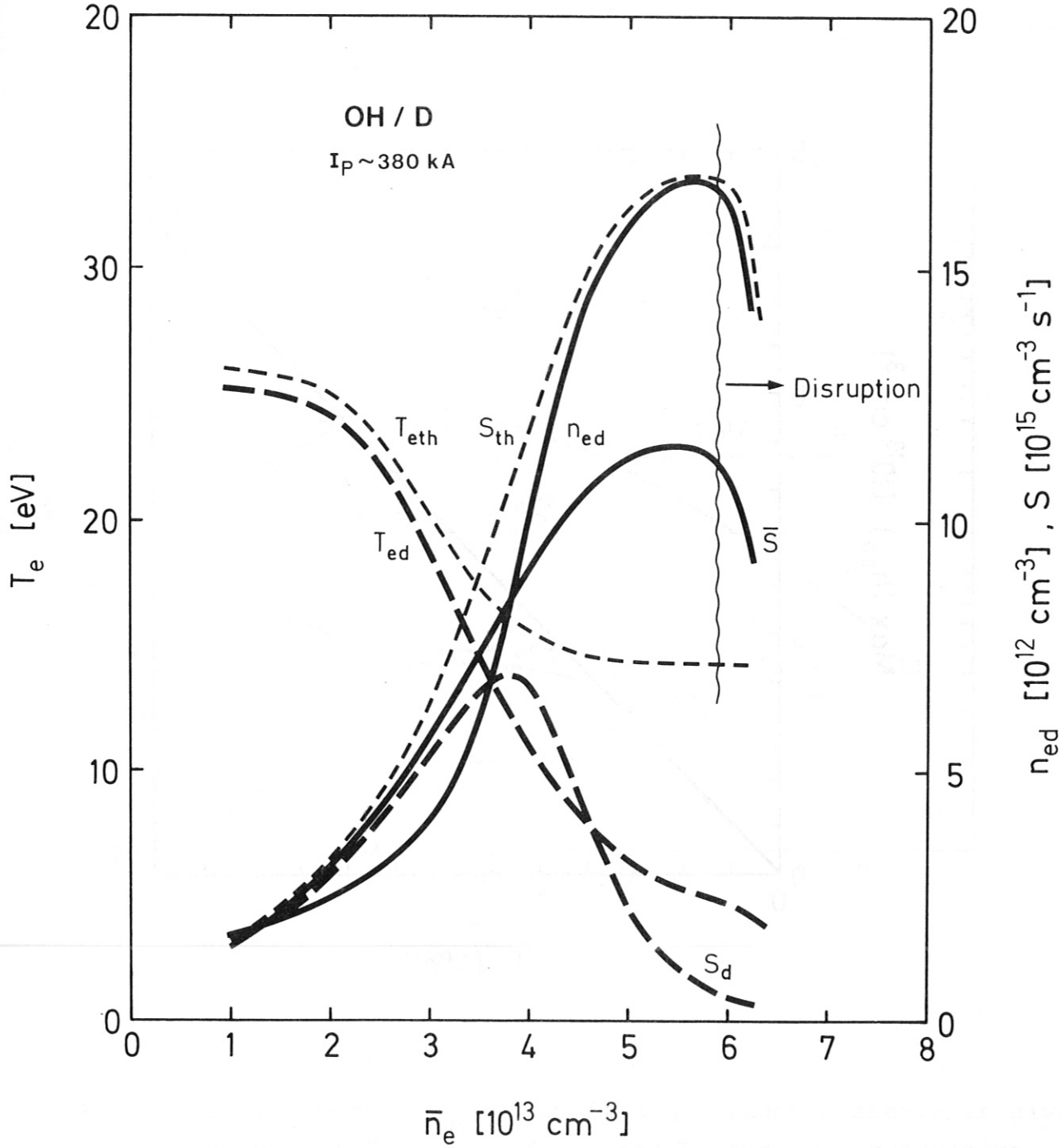


Fig.11: Production rate S of $D^+$. $T_{ed}$ and $n_{ed}$ are the measured electron temperature and density near the divertor plate. $T_{eth}$ is the calculated electron temperature at the divertor throat. $S_d$ and $S_{th}$ are the production rates near the divertor plate and at the throat. $\bar{S}$ is the corresponding average value in the divertor. $\bar{S}$ is consistent with the total particle loss flux calculated from the measured ion saturation current $i_s$.

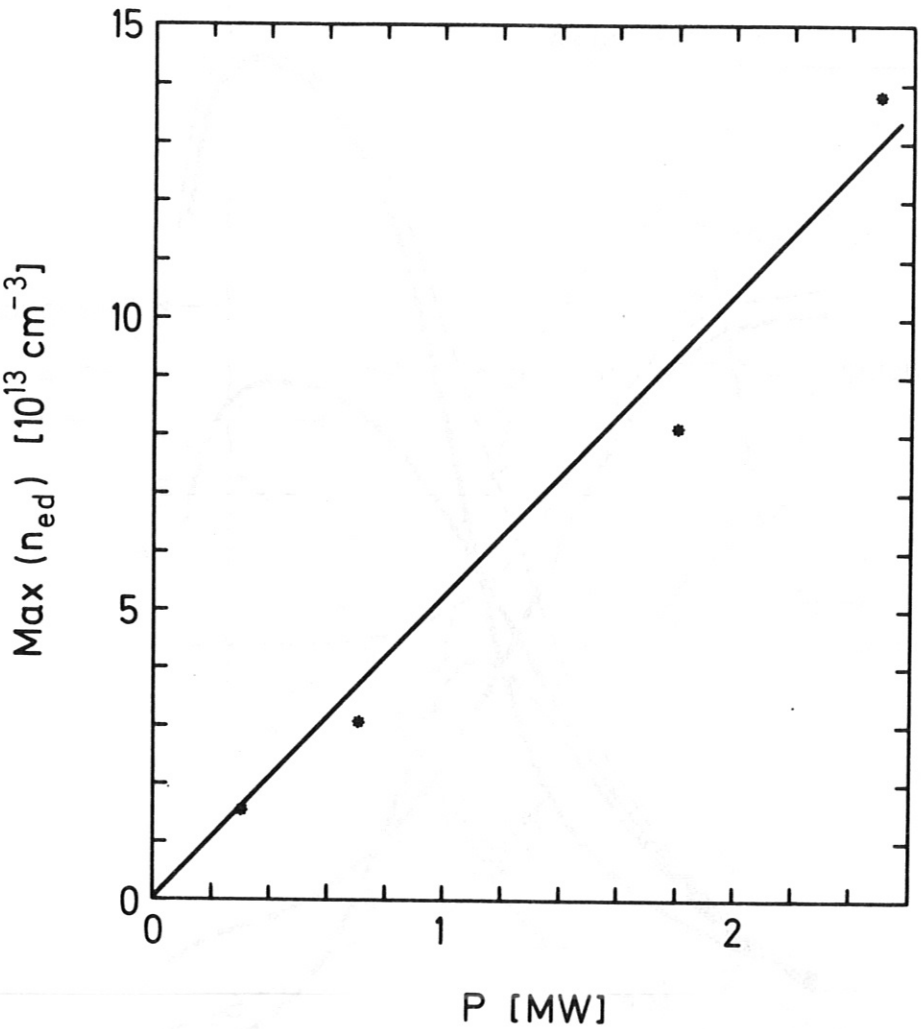


Fig.12: The observed maximum density $n_{ed}$ near the divertor plate versus heating power P with $P = P_{OH} + P_{NI}$.

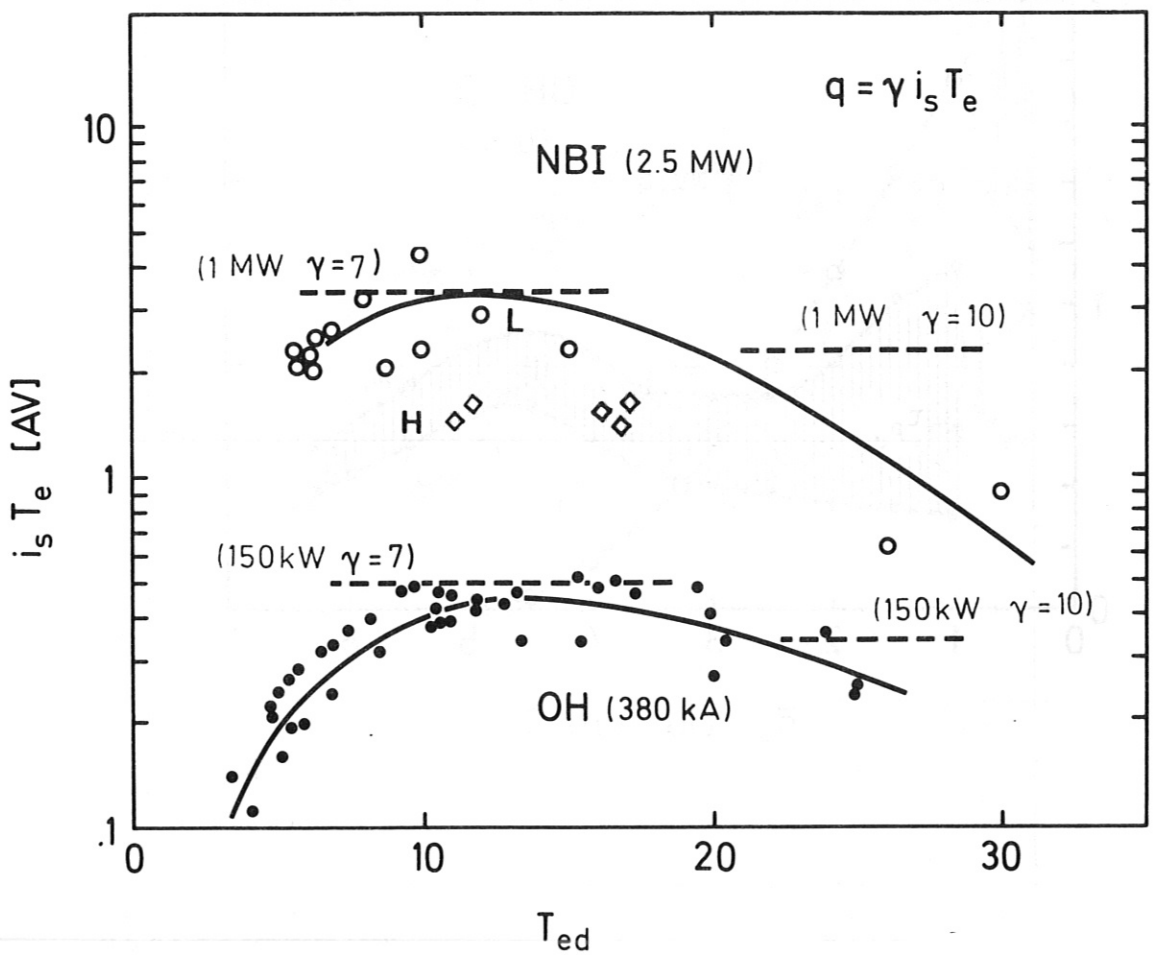


Fig.13: $i_s T_{ed}$ versus $T_{ed}$. Heat flux q through a sheath is given by $q = \gamma i_s T_e$ where $\gamma$, $i_s$ and $T_e$ are heat conduction rate, ion saturation current and electron temperature near the sheath. Dotted lines show values of $i_s T_{ed}$ which give total power losses onto the divertor plates of 1 MW and 0.15 MW, respectively for $\gamma = 7$ and $\gamma = 10$. (●) OH discharges, (O) L-type with $P_{NI} = 2.5$ MW and (◇) H-type with $P_{NI} = 2.5$ MW.

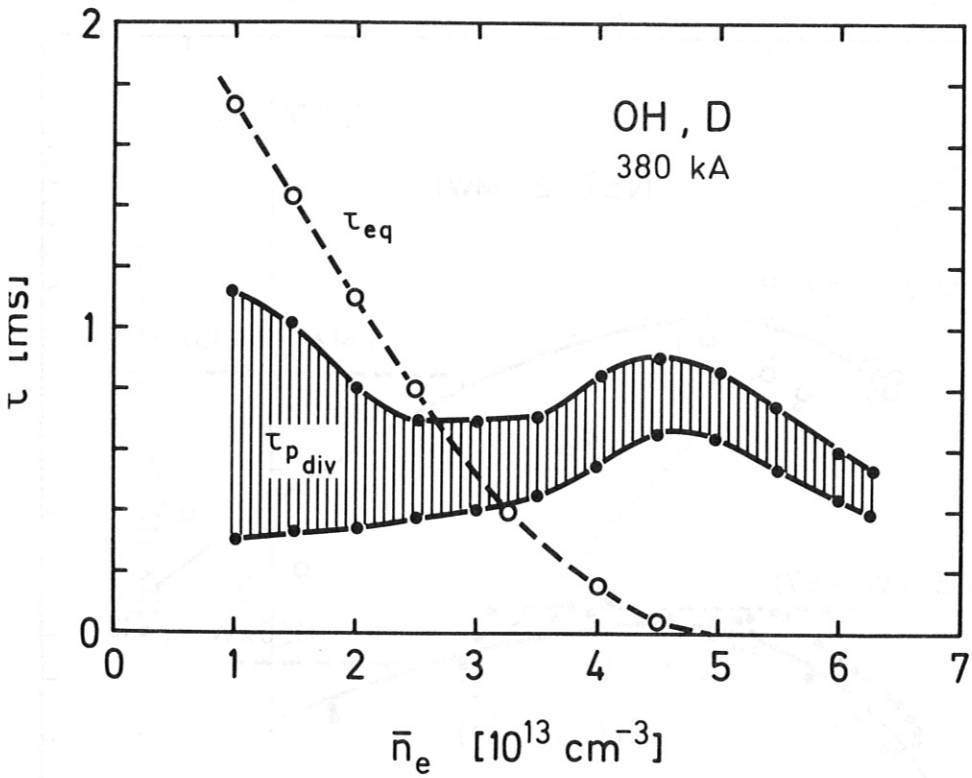


Fig.14: Equipartition time $\tau_{eq}$ and particle life time in the divertor $\tau_{pdiv}$. The particle life time in the divertor is given by $\tau_{pdiv} = N_{ed}/S$ where $N_{ed}$ is the total electron number in the divertor and S is the total particle source. S is calculated from Fig.11.

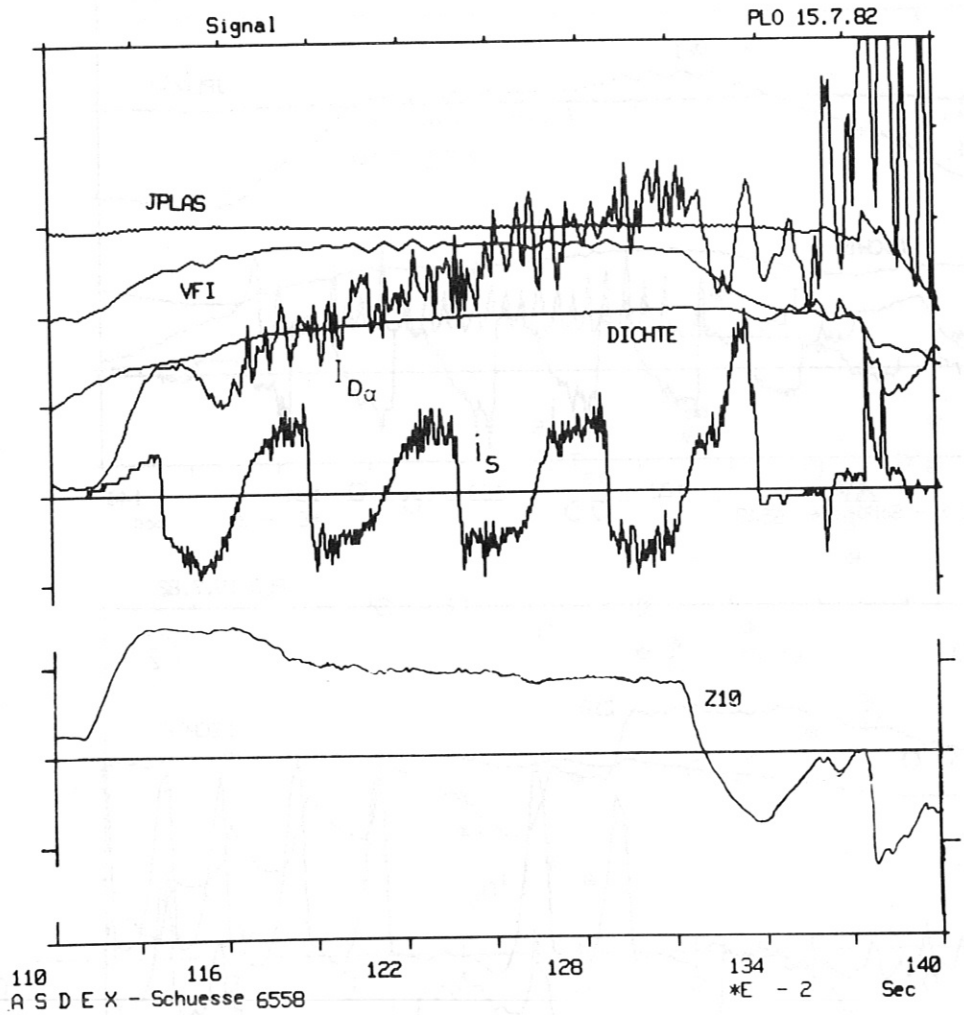


Fig.15: Fluctuations of ion saturation current $i_s$ during neutral beam injection (1.1 - 1.3 sec) in an L-type discharge

JPLAS: plasma current (100 kA/div)

VFI: vertical field coil current (10 kA/div)

DICHTE: mean electron density $\bar{n}_e$ ($2.4 \times 10^{13} cm^{-3}$/div)

$I_{D\alpha}$: $D_\alpha$ intensity in the divertor /16/

Z10: horizontal displacement (2 cm/div).

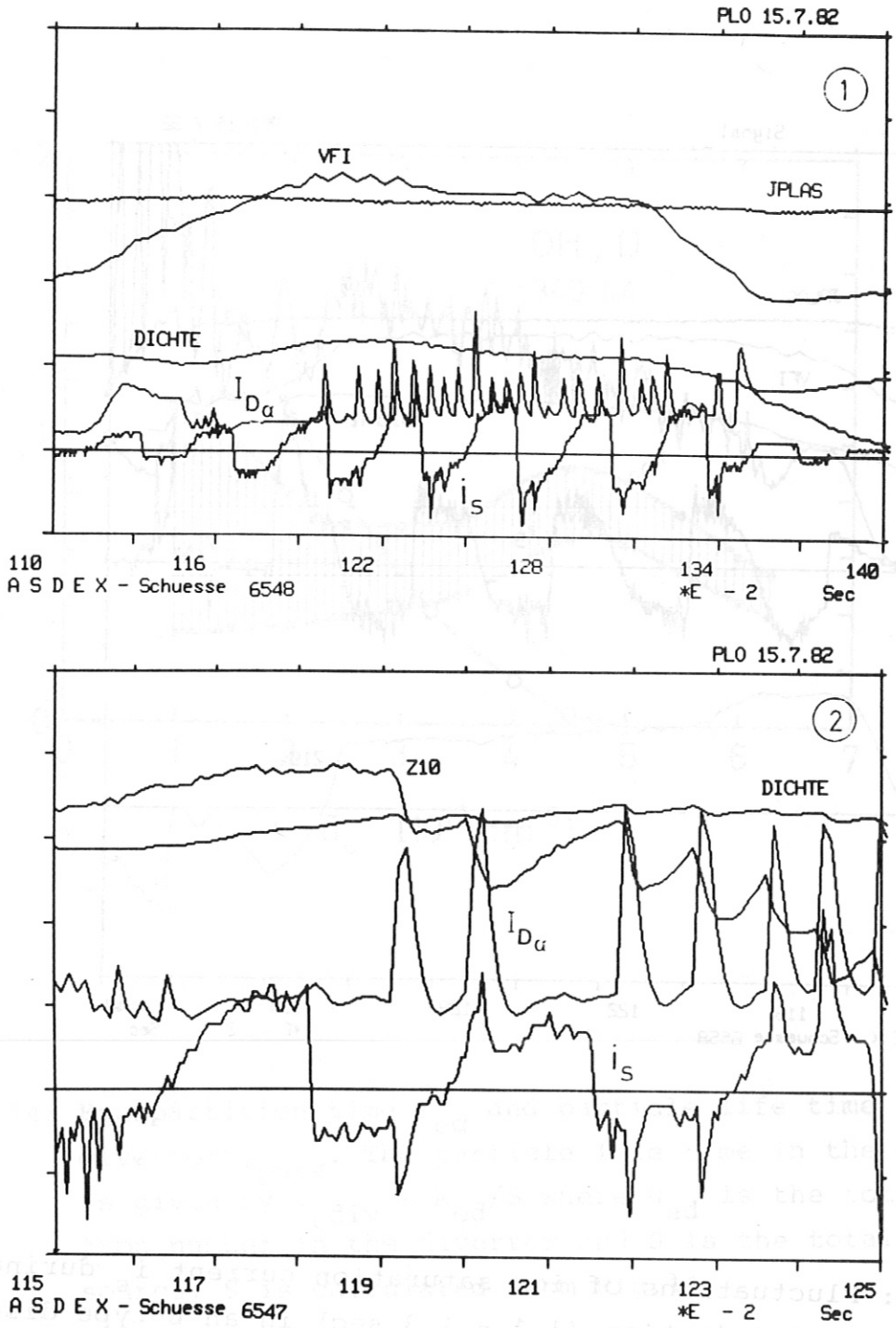


Fig.16: Fluctuation of ion saturation current $i_s$ during neutral beam injection (1.1 - 1.3 sec) in a H-type discharge. The meaning of JPLAS, VFI, DICHTE, $I_D$ and Z10 is the same as in Fig. 15.

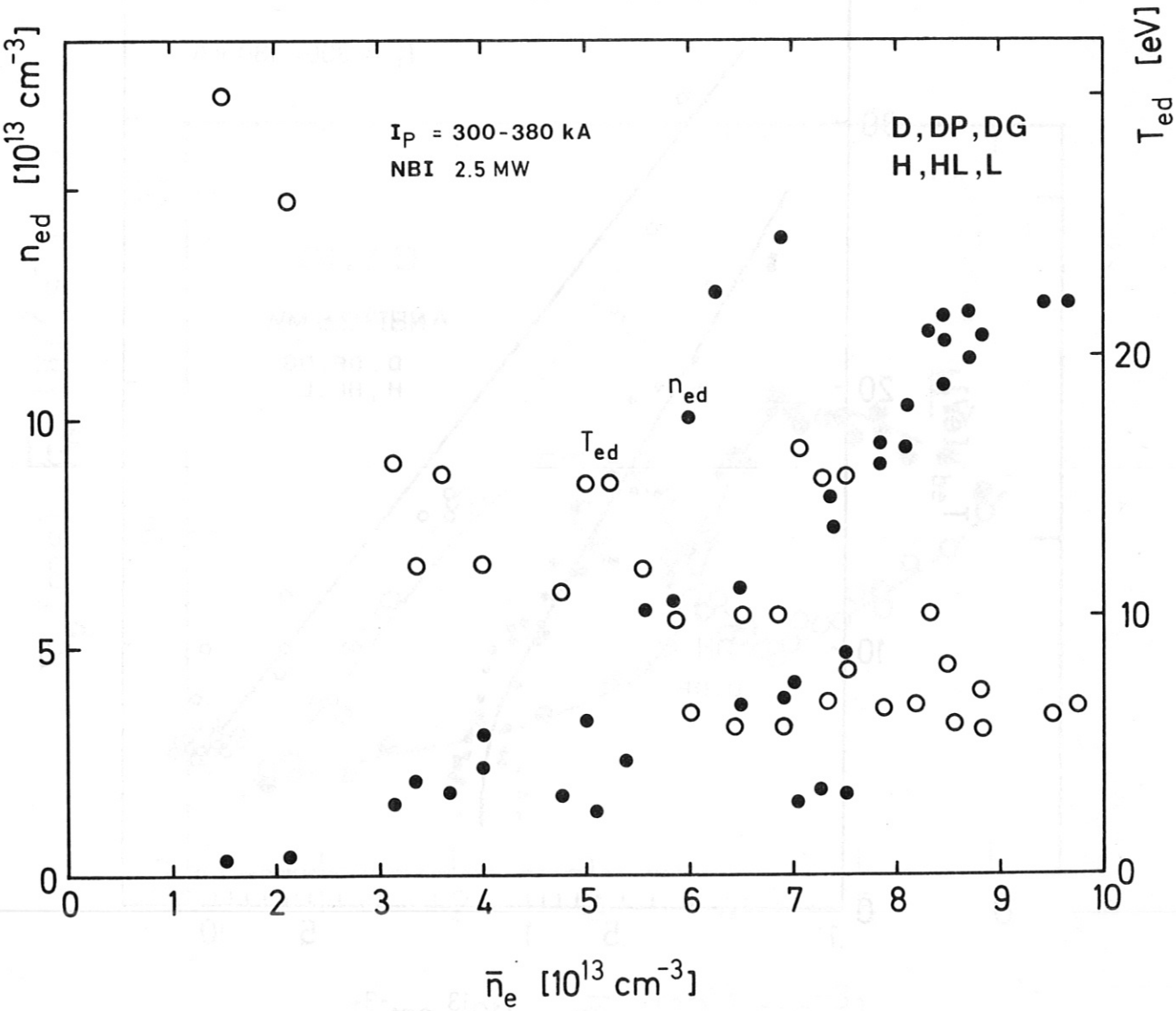


Fig.17: Electron temperature $T_{ed}$ and density $n_{ed}$ near the divertor plate for various discharge conditions.
D: normal divertor operation (no pumping)
DP: pumping in the divertor
DG: gas puffing in the divertor
H: H-type discharge
L: L-type discharge.

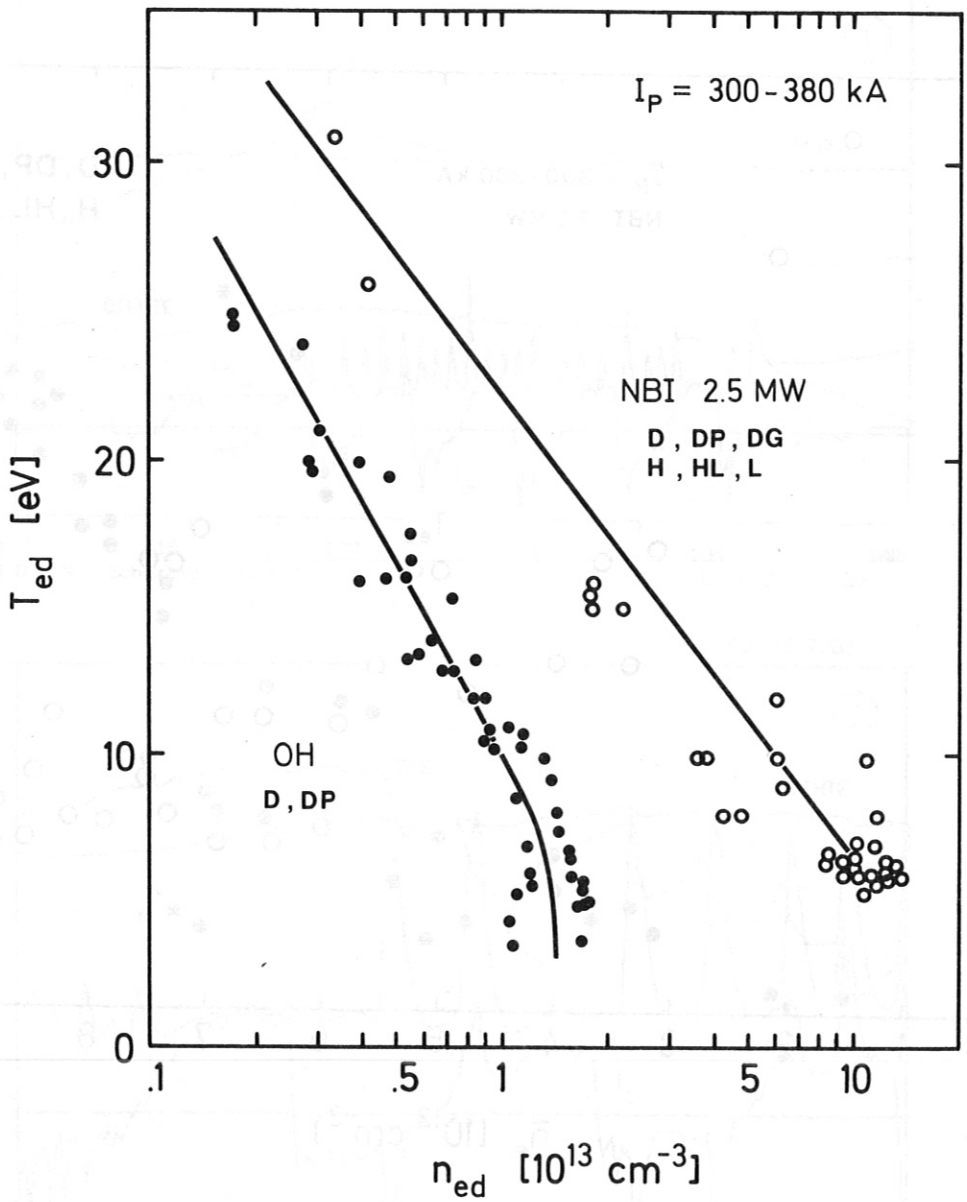


Fig.18: Electron temperature $T_{ed}$ versus density $n_{ed}$ with and without neutral beam injection. All data points shown in Fig. 17 are included.

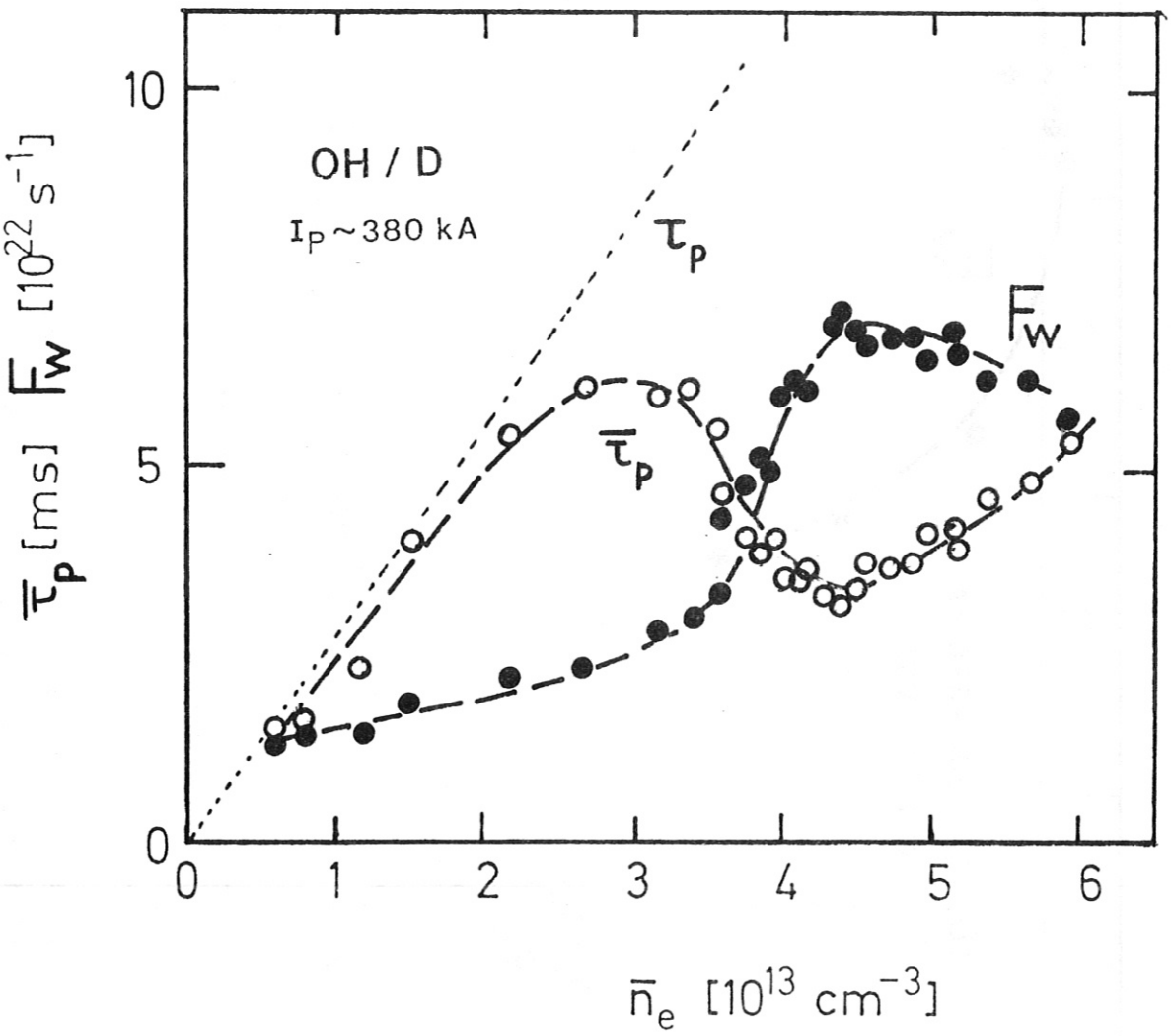


Fig.19: Overall particle confinement time $\bar{\tau}_p$ for ohmic discharges. $\bar{\tau}_p = N_e/F_w$, where $N_e$ and $F_w$ are the total electron number and total particle loss flux onto the first wall. $F_w$ is calculated by integrating the measured ion saturation currents $i_s$. $\tau_p$ is the particle confinement time in the main plasma. $\tau_p = N_{em}/F_D$, where $N_{em}$ and $F_D$ are the total electron number of the main plasma and the net particle loss flux into the divertor (or the net particle source in the main chamber).

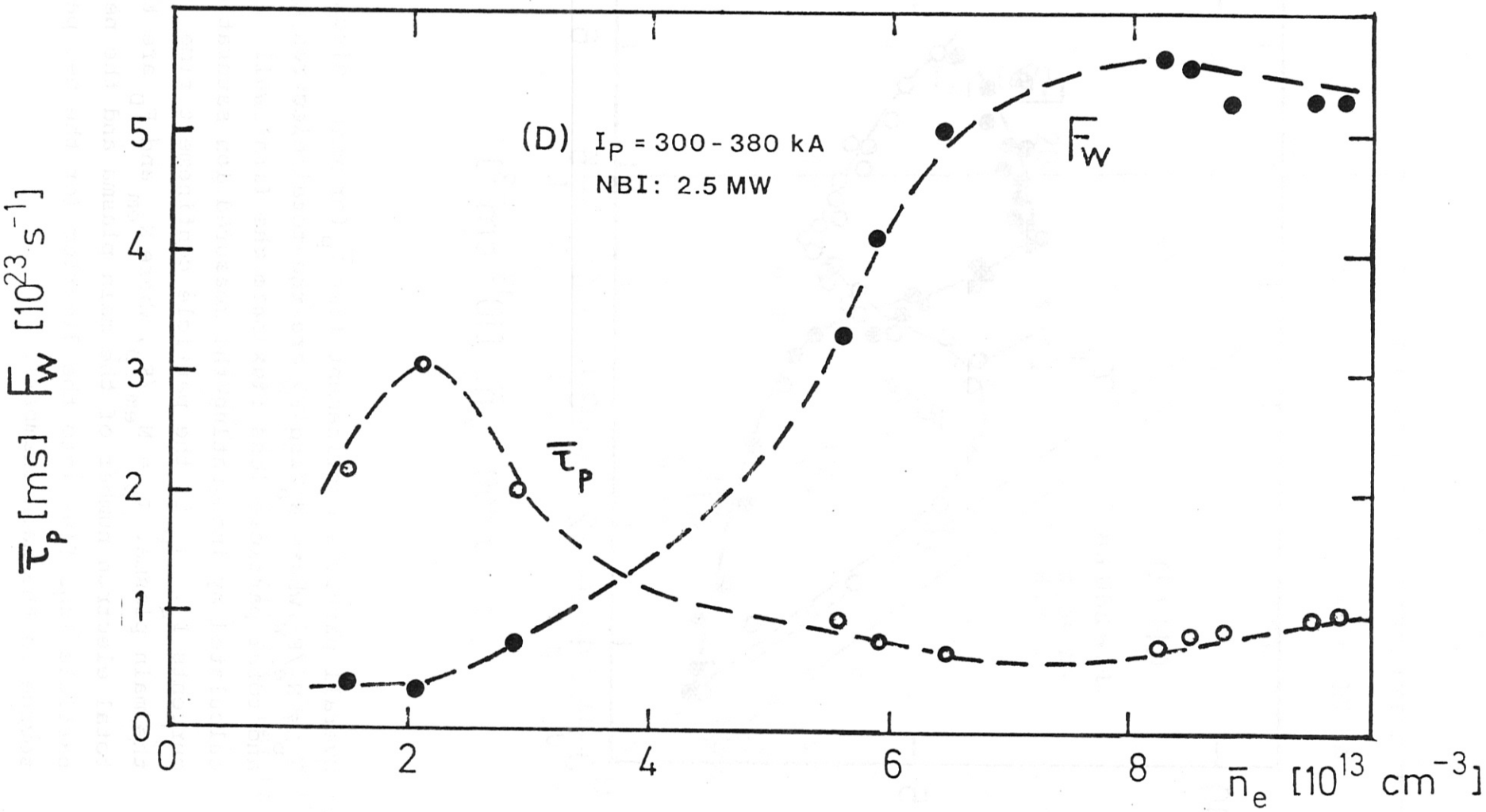


Fig.20: Overall particle confinement time $\bar{\tau}_p$ and total particle loss flux onto the first wall $F_w$.

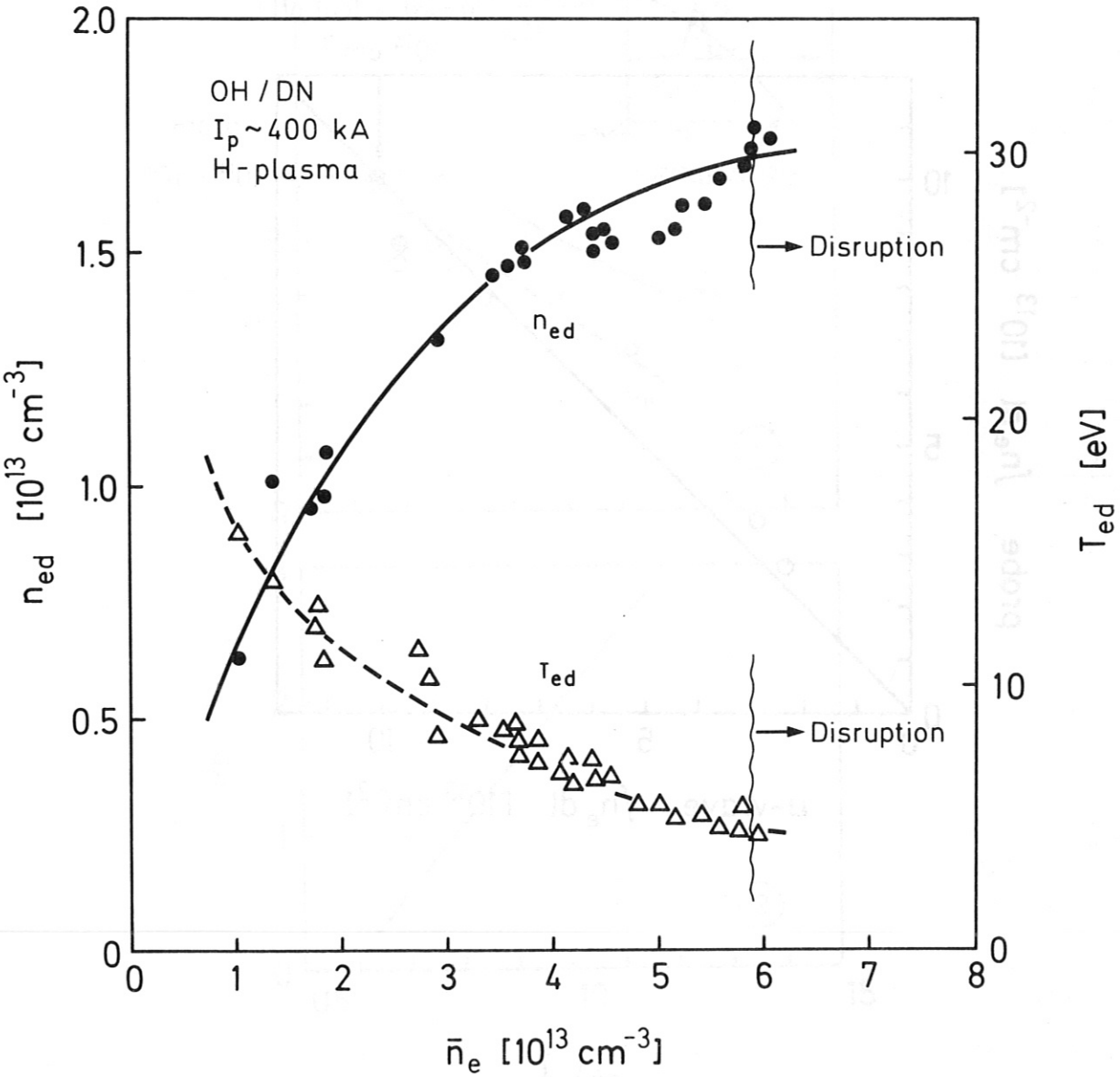


Fig.21: Electron temperature limitation in case of narrow divertor throat of 3.3 cm. (The normal throat width is 5.5 cm). The data are obtained with filling gas of $H_2$. The minimum electron temperature is around 5 eV and the maximum density around 1.7 x $10^{13}$ cm$^{-3}$. These values are similar to those with the normal divertor throat shown in Fig. 10.

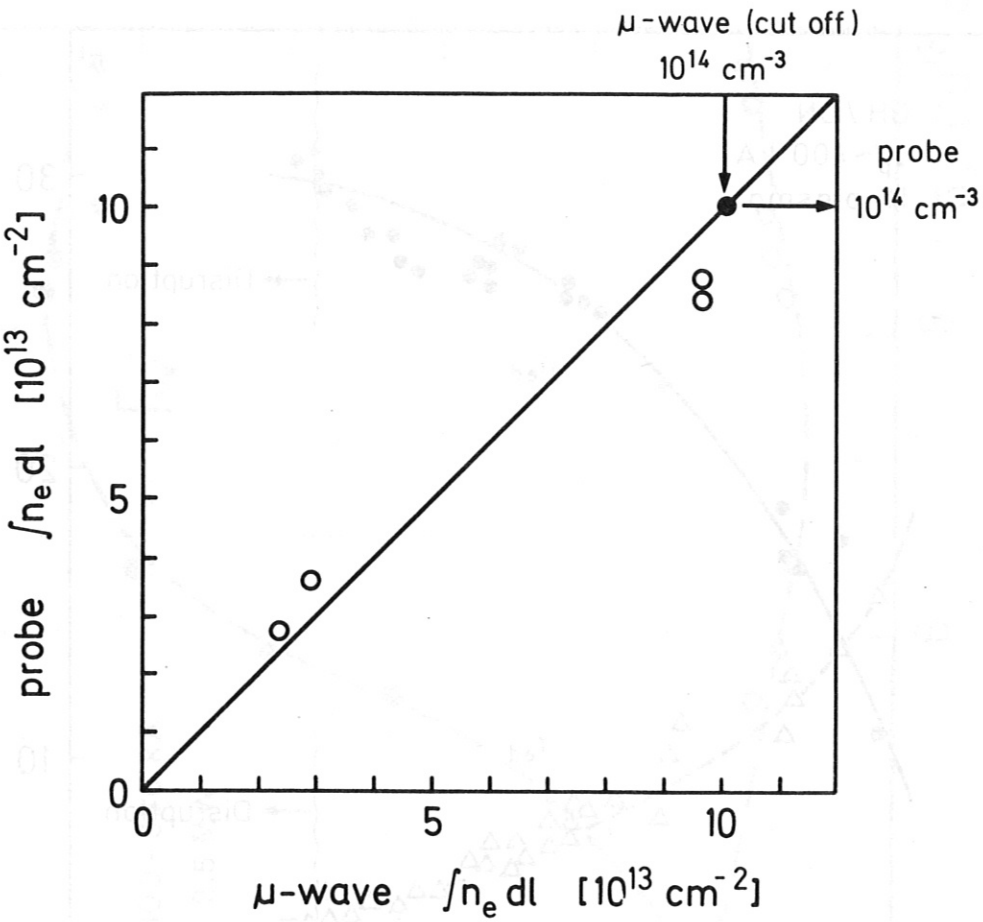


Fig.22: Absolute calibration of the density values obtained from probe measurements.

●: cut off density for 3.3 mm μ-wave

O: line density.

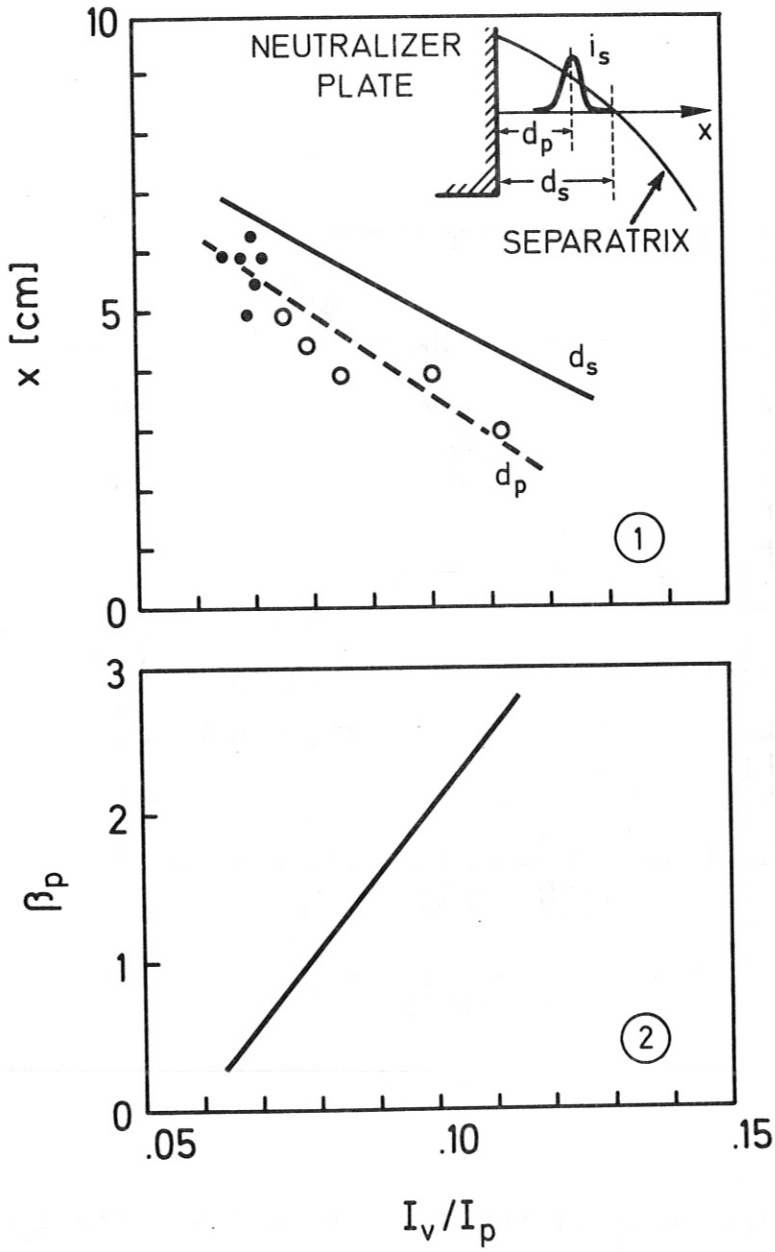


Fig.23: Position of the peak of divertor plasma profiles $d_p$ and position of the separatrix magnetic surface $d_s$.
$I_M/I_p$ = 0.1.
$I_M$: multi pole coil current
$I_p$: plasma current
$I_v$: vertical field coil current
$\beta_p$: poloidal ß assuming $l_i$ = 1.3
(——): calculated values
(●): measured values without NBI
(O): measured values with NBI

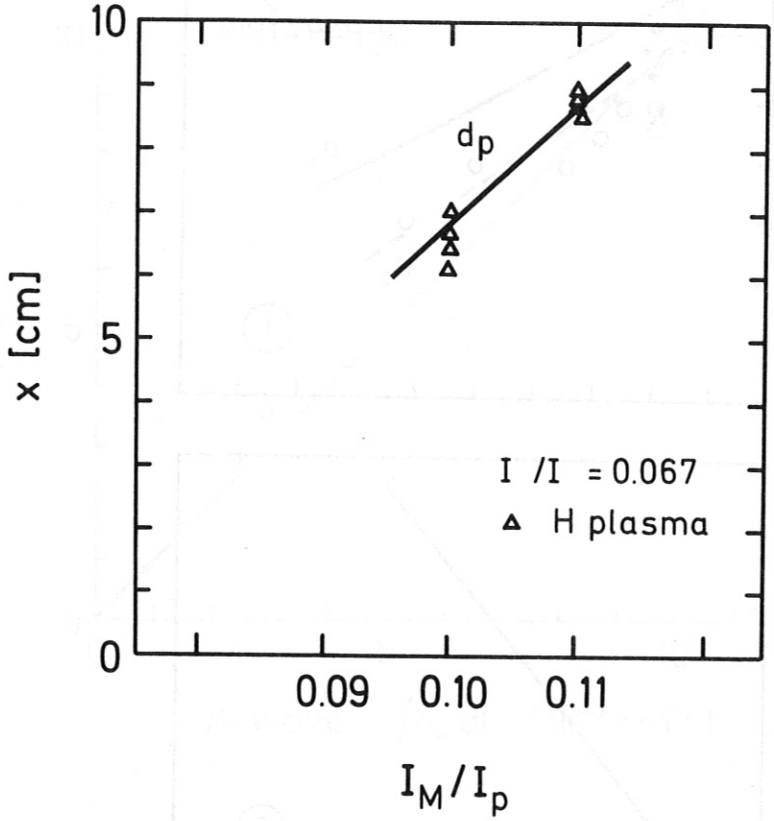


Fig.24: Peak position $d_p$ of the divertor plasma with $I_v/I_p = 0.067$. The meaning of X, $I_M$, $I_p$ and $I_v$ is given in Fig.21. These data are obtained in hydrogen discharges.

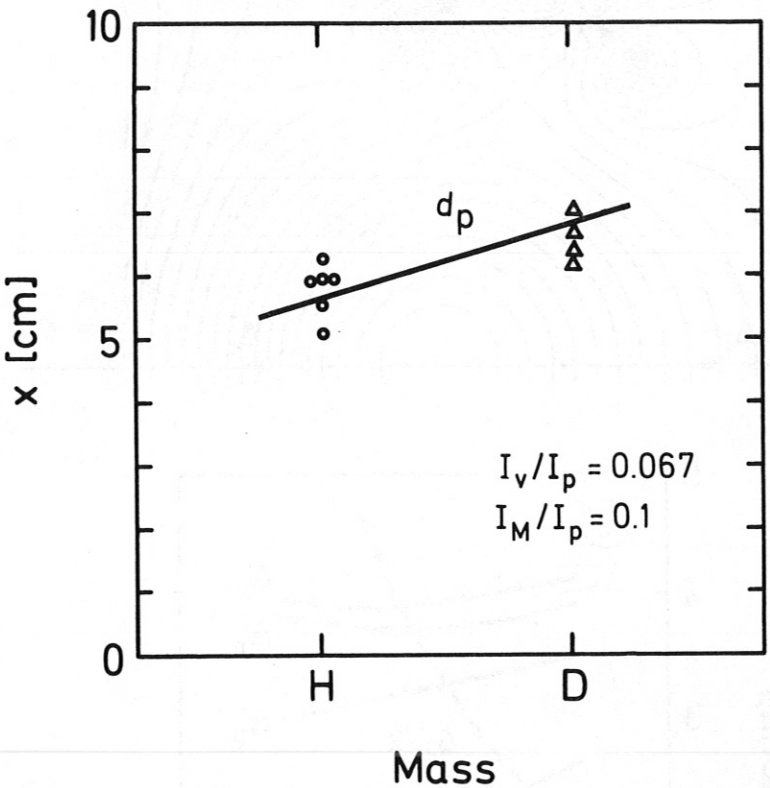


Fig.25: Peak positions $d_p$ of the divertor plasma in hydrogen and deuterium discharges with $I_M/I_p = 0.1$ and $I_v/I_p = 0.067$.

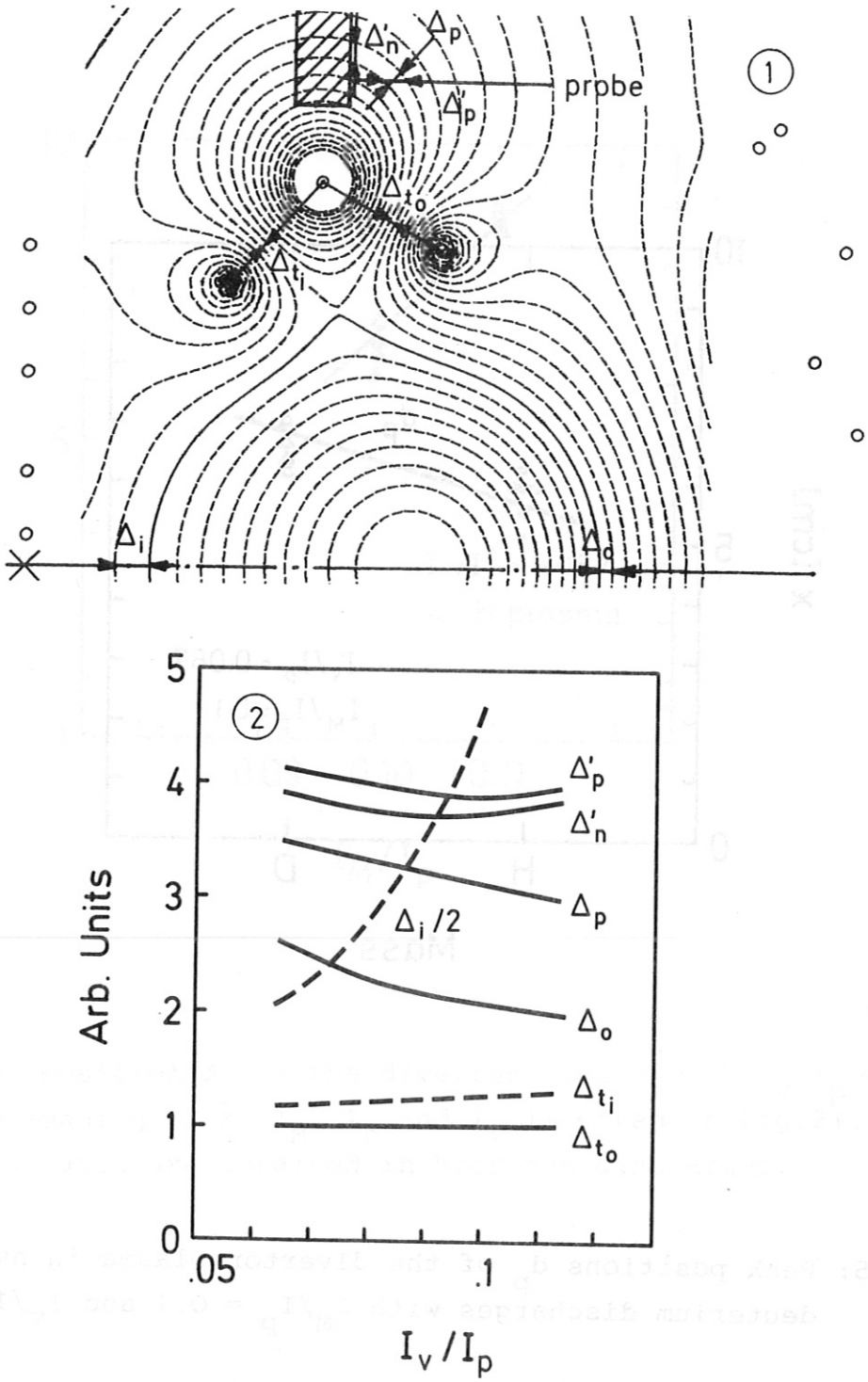


Fig.26: Geometrical factors for a divertor configuration with $I_M/I_p$ = 0.1 The meaning of $I_M$, $I_p$ and $I_v$ is the same as in Fig.23.